

# Preservation of compound delta in the rapidly subsiding Pliocene Orinoco Delta: Insights from quantitative fluvial, tidal and storm-wave signals

Yang Peng<sup>a,b,\*</sup>, Ronald J. Steel<sup>c</sup>, Cornel Olariu<sup>c,d</sup>, Shunli Li<sup>e</sup>

<sup>a</sup> Hainan Institute of China University of Petroleum (Beijing), Sanya, 572025, China

<sup>b</sup> College of Geosciences, China University of Petroleum (Beijing), Beijing, 102249, China

<sup>c</sup> Department of Geological Sciences, The University of Texas at Austin, Austin, TX, 78712, USA

<sup>d</sup> National Institute for Marine Geology and Geoecology, Bucharest, 024053, Romania

<sup>e</sup> School of Energy Resources, China University of Geosciences, Beijing, 100083, China

## ARTICLE INFO

### Keywords:

Compound clinoform

Channel

Mouth bar

Wave- or tide-influenced distributary channel

Mixed-influence mouth bar

Wave-dominated deposit

## ABSTRACT

Despite the documentation of compound clinoform morphology in modern deltas over the past two decades, there is still a scarce recognition of these in the stratigraphic record. Among the ancient cases that have been recognized, tide- and wave-dominated compound clinoforms have been documented. Here we present a fluvial- and wave-dominated compound clinoform delta in the Pliocene Orinoco Moruga Delta on Trinidad. The outcrops exhibit lateral variation with wave-dominated and mixed-influence deltaic clinoforms preserved in the proximal (i.e., upstream) part (SSW) of the compound system and wave-dominated deltaic clinoforms in the distal (i.e., downstream) part (NNE). The shoreline clinoforms are 5–15 m thick, sandy coarsening-upward units, and they commonly comprise HCS/SCS and wave-rippled sandstones generated by storm wave processes in both upstream and downstream parts. In the upstream part where the deposition location was close to main sediment supply, the shoreline clinoforms comprise an upper unit of fluvial-dominated mouth bar and channel deposits overlying a lower unit of mixed-influence mouth bars and wave-to tide-influenced channel deposits. The subaqueous clinoforms are 30–50 m thick and are characterized by coarsening-upward units changing from thick, bioturbated siltstones and mudstones at lower levels, through interbedded siltstones/mudstones and thin hummocky/swaley cross-stratified (HCS/SCS) sets, to occasional amalgamated HCS/SCS beds. The subaqueous clinoforms in these proximal and upstream parts are somewhat sandy and notably influenced by wave processes. In contrast, the distal parts of the subaqueous clinoforms are muddy with repetitive, frequent thin beds of both HCS or wave-rippled beds and especially wave-enhanced sediment gravity flow deposits. The compound clinoform delta in the Moruga Formation thus exhibits a spectrum of fluvial, tidal, and storm-wave signals, along with diverse channel types. This variability provides a valuable opportunity to document the interactions among river, tidal, and storm-wave processes as well as delta building processes driven by the various types of channels within the compound clinoform delta.

## 1. Introduction

Compound clinoforms in modern deltas have been well documented from their bathymetric morphology (Fig. 1 in Peng et al., 2020). They comprise a shoreline-attached clinoform and a coeval subaqueous clinoform connected by a subaqueous platform (Pirmez et al., 1998; Driscoll and Karner, 1999; Swenson et al., 2005; Patruno and Helland-Hansen, 2018; Pellegrini et al., 2020). Many modern deltas, such as Ganges-Brahmaputra, Gulf of Papua, Mahakam, Yangtze, Amazon delta, Atchafalaya shelf and Po-Adriatic, exemplify this

compound geometric configuration (Cattaneo et al., 2003; Roberts and Sydow, 2003; Walsh and Nittrouer, 2009; Patruno et al., 2015; Pellegrini et al., 2015). Modelling studies suggest that waves and marine currents interact with river-derived sediments to form the compound-clinoform morphology (Pirmez et al., 1998; Swenson et al., 2005; Willis et al., 2021). The generation of the subaqueous delta involves winnowing of sediment from the shoreline storage areas together with flood-bypass of sediment, and this is accompanied by multiple cycles of reworking and resuspension of sediment on the platform beyond the shoreline areas. It is therefore not surprising that the subaqueous delta tends to be

\* Corresponding author. Hainan Institute of China University of Petroleum (Beijing), Sanya 572025, China.

E-mail address: [ypeng@cup.edu.cn](mailto:ypeng@cup.edu.cn) (Y. Peng).

<https://doi.org/10.1016/j.marpetgeo.2025.107456>

Received 1 October 2023; Received in revised form 4 January 2025; Accepted 6 May 2025

Available online 15 May 2025

0264-8172/© 2025 Elsevier Ltd. All rights are reserved, including those for text and data mining, AI training, and similar technologies.

relatively fine-grained, reflecting the very high mud content of most river budgets (cf. Macquaker and Gawthorpe, 1993; Klausen et al., 2018). However, strong floods or cyclonic storms can also bring discrete intervals of coarser sand or thick mass-transport units onto the subaqueous delta (Palamenghi et al., 2011).

Recognition of compound-clinoforms has been documented in the ancient rock record (Hampson, 2010; Hampson and Premwichein, 2017; Peng et al., 2018a; Rossi et al., 2019). The Havert Formation in the Barents Sea was interpreted as a compound-clinoform delta with its shoreline clinoform and inner subaqueous platform dominated by fluvial, wave and tidal processes, and outer subaqueous platform to subaqueous foreset dominated by fluvial floods and storm waves (Rossi et al., 2019). A mixed fluvial and tidal compound clinoform delta was recognized in the Deguynos Formation of the Pliocene Colorado delta using an integration of measured sections, 3D photomosaics and modern Colorado delta analogue (Rey et al., 2022). The Lower Morne L'Enfer Formation of the Pliocene Orinoco delta has been interpreted to preserve compound-clinoform strata produced by mixed influence of tidal and wave processes (Osman et al., 2023).

The presence of compound-clinoform deltas in the ancient record implies that some traditional interpretations of stratigraphy need to be reconsidered. Specifically, the vertical stacking of various facies exhibiting lithological changes, previously interpreted as a result of variations in relative sea level or sediment supply, may in fact result from a single regression cycle. The subaqueous clinothems displaying well-developed platform-to-foreset rollover may have been mis-interpreted as shoreline clinothems (Steel et al., 2020), leading to an overestimation of allogenic cycles in stratigraphic analyses (Peng et al., 2020a). Some relatively muddy coarsening-upward packages containing thin beds of

hummocky/swaley cross-stratified (HCS/SCS) strata, typically interpreted as shoreface deposits (i.e., shoreline clinothem) (Peng et al., 2020b), can also occur in the proximal reaches of the subaqueous clinothems. This reinterpretation can be justified by a careful examination of overall stacking patterns and succession thickness (cf. Steel and Olsen, 2002; Helland-Hansen and Hampson, 2009).

Mixed-influence deltas tend to form compound clinoforms where wave, tidal and combined-flow currents with high near-bed shear stress interact with the river output. As well as directly aiding outflow, these currents can erode, rework and bypass relatively fine-grained sediment basinward, resulting in sediment partitioning between the two clinoforms (Pirmez et al., 1998; Swenson et al., 2005; Walsh and Nittrouer, 2009; Hampson and Premwichein, 2017; Peng et al., 2018a, 2020a). Nonetheless, there remains a notable gap in understanding the depositional dynamics within such settings. In particular, the subaqueous deltas, situated at depths ranging from a few meters to 10s of meters, need more study to understand their active deposition induced by significant storms, river-derived hyperpycnal/hypopycnal flows or other currents (e.g., Kuehl et al., 1997; Michels et al., 1998; Cattaneo et al., 2003; Zăinescu et al., 2019). The Moruga Formation was previously interpreted as a stacked series of delta fronts influenced by mixed fluvial, wave, and tidal processes (Peng et al., 2020b). However, the present study re-evaluates the strata as the deposits of a compound-clinoform delta. A range of fluvial, tidal and storm-wave signals have been systematically identified and documented within this system. Additionally, fluvial-dominated and wave-to tide-influenced channels have been observed at different locations. These findings contribute to elucidating the diversity of mechanisms involved in the formation of the compound clinoform deltaic system.

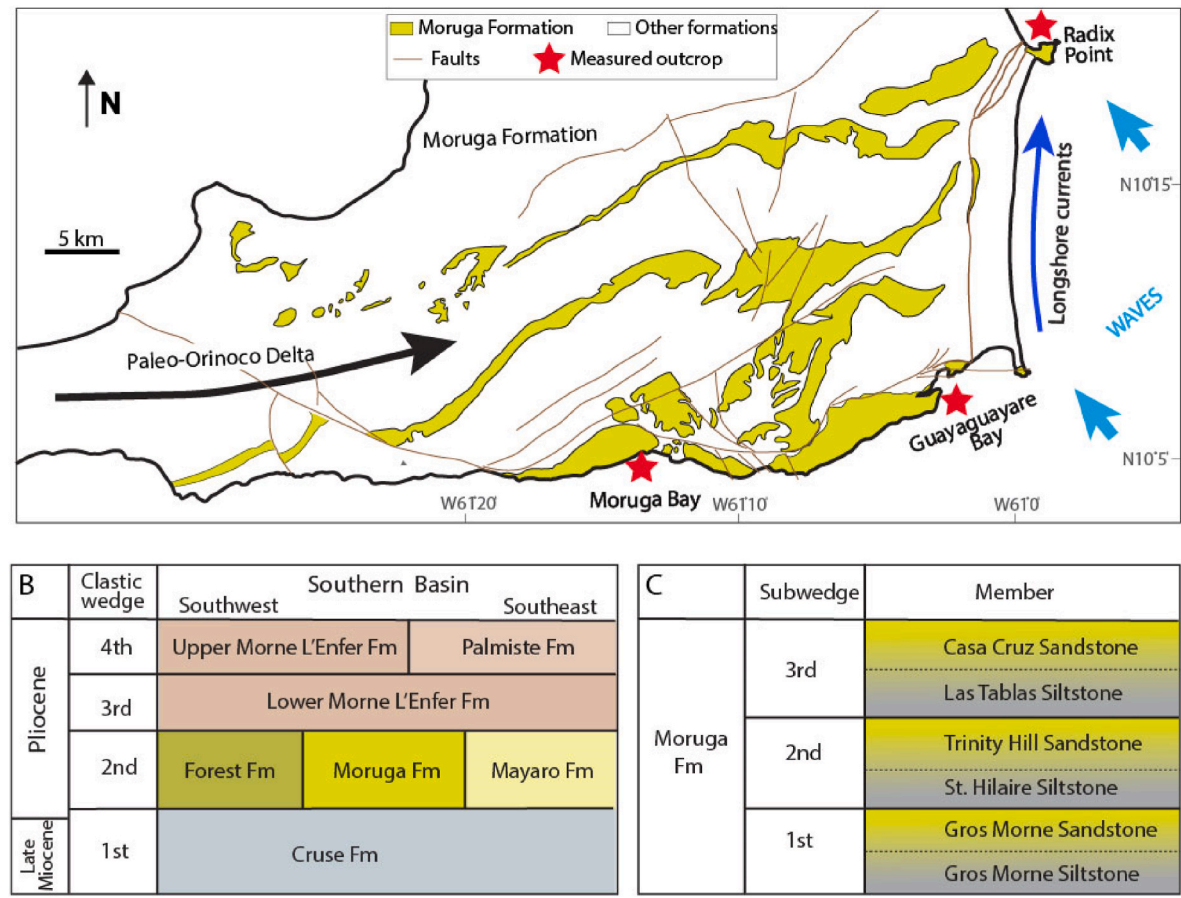


**Fig. 1.** (A) Outcrop distribution of the Moruga Formation on south Trinidad (after Kugler, 1959) with locations of study areas at Guayaguayare Bay, Radix Point and Moruga Bay. (B) Stratigraphic column for the four clastic wedges from the late Miocene to Pliocene. (C) The Moruga stratigraphy consisting of three subunits built during three major deltaic growth stages.

## 2. Geological setting

Trinidad is located at the junction of the Venezuela-Columbus Foreland Basin which was mainly constructed by the Orinoco River and its delta from the late Miocene to the present (Mann et al., 2006; Escalona and Mann, 2011; Castillo and Mann, 2021). In the meanwhile, Trinidad lies within a plate-boundary zone where the Caribbean Plate moved eastward and collided with the South American Plate (Alvarez et al., 2021). North-south compression between the two plates during the latest Pliocene and Pleistocene led to deformation and uplift of previously deposited sedimentary strata on Trinidad. As such, an east-west depositional dip transect through the shelf-margin sedimentary prism outcropped along the southern Trinidad coast (Fig. 1).

During the late Miocene to Pleistocene, repeated cross-shelf transits of the paleo-Orinoco River and its large delta system built four large-scale clastic wedges (i.e., thick sand-prone, strongly progradational intervals) (Fig. 1) (Chen et al., 2018). The studied Moruga Formation (coeval with Forest/Mayaro formations) represents strata of the second clastic wedge (early-mid Pliocene) and is characterized by wave-dominated processes and river influences (Peng et al., 2017, 2020b). The Moruga Formation is further subdivided into three sub-wedges: (1) the Gros Morne Siltstone and Gros Morne Sandstone members, (2) the St. Hilaire Siltstone and Trinity Hill Sandstone members, and (3) the Las Tablas Siltstone and Casa Cruz Sandstone members (Fig. 1). These sub-wedges were built by multiple episodes of deltaic growth across a rapidly subsiding shelf, and a resultant 1200 m thick succession was documented in Peng et al. (2020b). In this study, the upper two sub-wedges that were deposited in shallow-marine shelf settings are further documented in detail.

## 3. Methodology

The 1200 m-thick Moruga Formation strata were previously documented and analyzed including the use of photomosaics (Peng et al., 2020b). The outcrops are located at Guayaguayare Bay, Moruga Bay, Radix Point and Galeota Point on southern and southeastern Trinidad, and they are mostly oriented subparallel to the regional depositional dip. We present the details of two well-exposed outcrops of the Moruga Formation situated at Guayaguayare Bay and Radix Point (Fig. 1). 270 m of the Trinity Hill Sandstone Member (Fig. 2) and 240 m of the Las Tablas Siltstone-Casa Cruz Sandstone members were measured at these locations. Cm-to dm-scale observations on bed thickness, bedding contact, grain size, sedimentary structure, organic matter/plant fragment, trace fossil with Bioturbation Index (BI) (Taylor and Goldring, 1993) were recorded in order to characterize facies variability.

Along with the conventional stratigraphic measured section, a sedimentary process histogram was constructed using the methodology of Rossi et al. (2017). In this approach, each measured bed or bedset was assigned three percentages, reflecting probability of its formation being influenced by waves, tides, or fluvial processes, respectively. Although fluvial processes predominantly occur in subaerial environments, their influence also extends into subaqueous deltas through mechanisms such as high sediment supply, extension of channels into subaqueous delta as distributary channels, and river-flood as hyperpycnal flows. The resulting sedimentary, mixed-process histogram provides insights into the interactions among the three process components that contributed to the formation of stratigraphy through geological time (Fig. 2). Note that wave and tidal processes not only interact by reworking but also directly aid fluvial output by allowing it to persist farther into the subaqueous delta (Wright and Friedrichs, 2006; Steel et al., 2024). This method was applied on the measured section from Guayaguayare Bay because it demonstrates an interesting record of mixed-energy depositional processes. The other succession from Radix Point was dominated by wave processes and conventional description method was therefore used (Fig. 3). The interpretations of compound clinoform subenvironments were based on descriptions of measured sections, calculated process

percentages, and the stacking patterns of associated facies (see details in Section 4) (Fig. 2).

## 4. Results

### 4.1. Depositional facies

The Moruga Formation comprises six facies associations (FA) deposited in a shallow marine setting (Table 1). Since most of the FAs have been previously documented by Peng et al. (2020b), they are briefly described here, with a focus on re-interpretation based on the new recognition of a compound clinoform setting (cf. Peng et al., 2020b).

#### 4.1.1. Facies association 1: siltstones and mudstones with thin sandstone beds

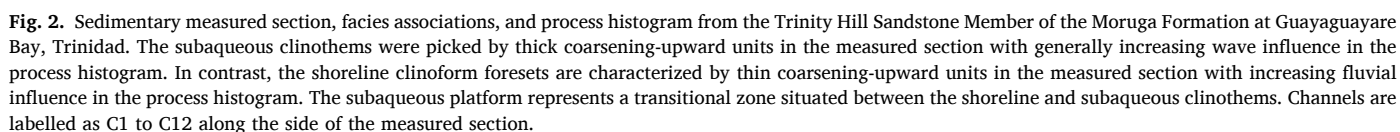
**Description.** FA1 consists of muddy successions that comprise laminated mudstone/siltstone beds (Fig. 4) with occasional thin, wave-rippled sandstones. FA1 is subdivided into FA1-1 and FA1-2 based on stratigraphic positions. FA1-1 is a very thick (10 m–15 m) muddy succession commonly underlying heterolithic wave-dominated deposits of FA2 (Fig. 2). Bioturbation of FA1-1 is moderate to intense (BI = 3–5) with occurrence of *Planolites* (P), *Chondrites* (Ch), *Skolithos* (Sk), *Phycosiphon* (Ph) (Figs. 2 and 3). FA1-2 units are 5–7 m thick with rare to no bioturbation (BI = 0–1) and are overlain by stacked river mouth bars (FA3) and mixed-influence mouth bars and sandy deposits (FA4) (Fig. 2).

**Interpretation.** FA1-1 is interpreted as deposits on the bottomsets of the subaqueous delta. The presence of moderate to intense bioturbation supports the interpretation of the basinal location, characterized by a notable absence of fluvial influence (cf., MacEachern et al., 2005). The thin wave-rippled sandstone beds in the muddy successions indicate that the bottomset was occasionally affected by influx of sediment due to large storm waves. The siltstones and mudstones of FA1-2 with only rare bioturbation are interpreted as muddy deposits that formed on the bottomset of the shoreline clinoform and innermost platform during fairweather conditions or weaker storm wave events. The rare bioturbation within FA1-2 suggests a stressed condition likely attributed to the proximity of fresh river water.

#### 4.1.2. Facies association 2: wave-dominated deposits

**Description.** FA2 is marked by HCS/SCS strata and wave-ripple laminated sets (3–5 cm thick) and common interbedded with mudstones. FA2 is subdivided into FA2-1, FA2-2 and FA2-3 based on the overall grain size and different stratigraphic locations. FA2-1 are relatively muddy with thin, lower very fine-grained sandstones, and they form a coarsening- and thickening-upward succession (30–50 m thick) together with underlying FA1-1 (Figs. 2 and 3). In the upper part of the FA2-1 succession there are amalgamated HCS/SCS sandstones (up to 2–3 m thick) (Fig. 4A). The lower part of the succession is characterized by muddy beds (0.1–0.7 m thick) interbedded with HCS/SCS beds (0.1–0.5 m thick, up to 10 m in wavelength) sandstones (Fig. 4B and C). At Radix Point, muddy, normally graded beds (up to 5 cm thick) associated with wave-rippled sandstones (Fig. 4F and G) are frequently observed in the FA2-1 (Fig. 3). The heterolithic intervals exhibit higher-diversity and higher-abundance trace-fossil suite (BI = 3–6) including *Ophiomorpha* (O), *Thalassinoides* (Th), *Skolithos* (Sk), *Teichichnus* (Te), *Planolites* (P), *Chondrites* (Ch), *Phycosiphon* (Ph), *Rosselia* (Ro), *Macaronichnus* (Ma), and *Diplocraterion* (Dp) at Radix Point (Fig. 4C, D, E, H, I) than those at the Guayaguayare Bay. FA2-2 is sandier and consists of upper very fine-grained HCS/SCS sandstones that are typically amalgamated to thicker units (up to 10–20 m thick) (e.g., 56–82 m in Fig. 2; 470–500 m in Fig. 3). FA2-3 exhibits some transition between FA2-1 and FA2-2, and comprises relatively thin amalgamated HCS/SCS or parallel-laminated sandstones interbedded with mudstone beds. Erosional surfaces are frequently observed in places. Occasionally, FA2-3 is







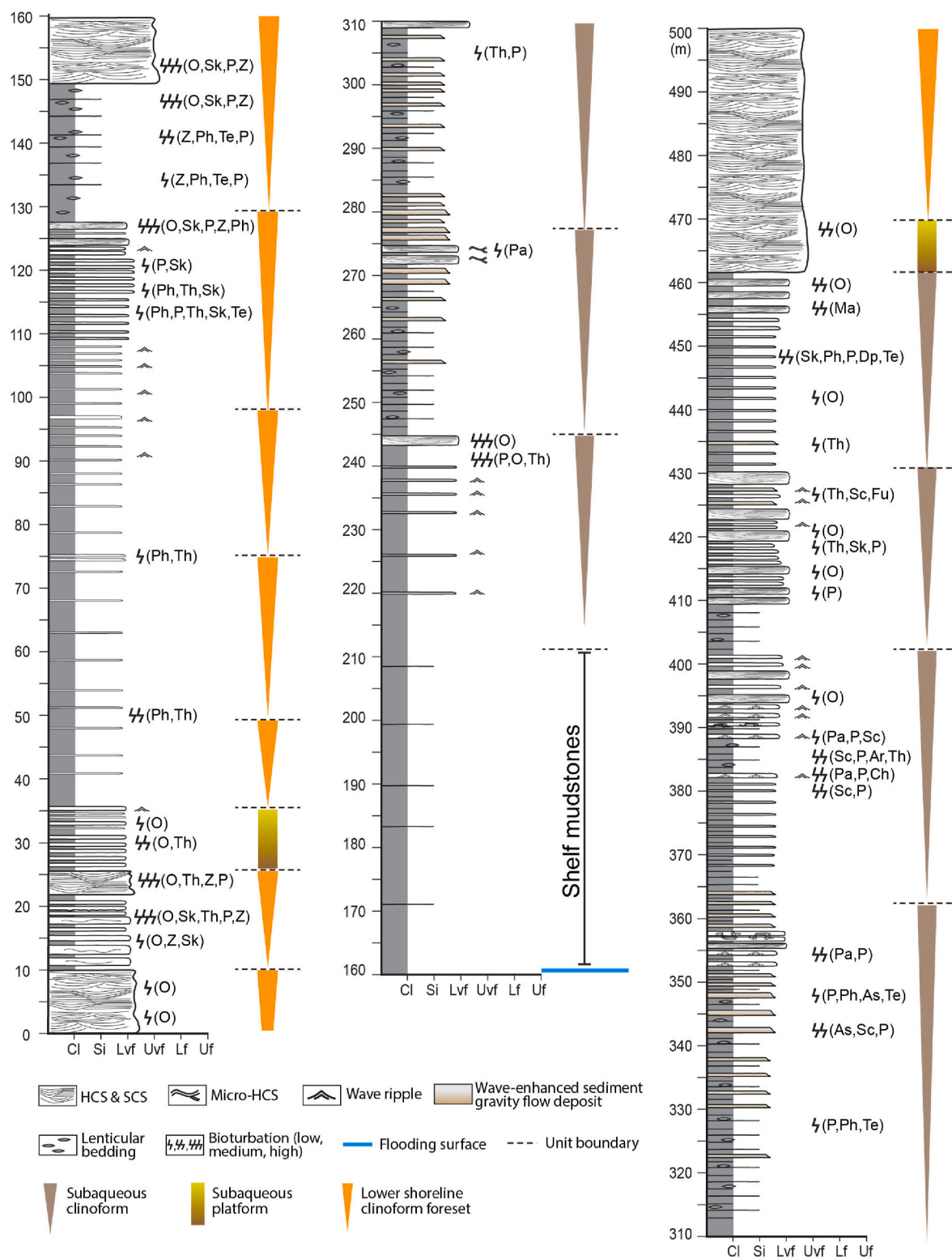


**Fig. 3.** Sedimentary measured section of the upper part of Trinity Hill Sandstone Member (0–160 m), Las Tablas Siltone Member (160–460 m) and lower part of Casa Cruz Sandstone Member (460–500 m) of the Moruga Formation at Radix Point showing several stacked units of subaqueous clinothems overlain by a subaqueous platform and shoreline clinothem. The boundaries of the subaqueous clinothems are picked at the muddiest bases, representing flooding surfaces onto which the subaqueous clinoform prograded. The shoreline clinothem is characterized by relatively thick deposits of lower-to upper-very-fine-grained sandstones, exhibiting amalgamated HCS/SCS probably due to high sediment supply and strong wave processes.

**Table 1**

Summary of facies associations in the Moruga compound clinoform delta.

Facies association	Bedding	Sedimentary structure	Stratigraphic position	Depositional environment
FA1: siltstones and mudstones with thin sandstone beds	Coarsening- upward; 10–15 m thick	Laminated mudstone & siltstone beds with thin, lower very fine- grained sandstones with HCS or wave ripples; moderately to intensely bioturbated (BI = 3–5) with the occurrence of <i>Planolites</i> , <i>Chondrites</i> , <i>Skolithos</i> , <i>Phycosiphon</i>	FA1-1 is 10–15 m thick and underlie heterotolithic wave-dominated deposits (FA2); FA1-2 is 5–7 m thick and overlain by river and mixed-influence mouth bars and sandy deposits (FA3-4)	FA1-1 are deposits on the subaqueous bottomset; FA1-2 are muddy deposits on the shoreline bottomset and
FA2: wave-dominated deposits	Coarsening- and thickening- upward; 15–50 m thick	FA2-1: Muddy intervals with thin beds of HCS/SCS sandstone and wave-enhanced sediment gravity flow deposits; highly bioturbated (BI = 3–6) with <i>Ophiomorpha</i> , <i>Thalassinoides</i> , <i>Skolithos</i> , <i>Teichichnus</i> , <i>Planolites</i> , <i>Chondrites</i> , <i>Phycosiphon</i> , <i>Roselia</i> , <i>Macaronichnus</i> , and <i>Diplocraterion</i> ; FA2-2: thick, amalgamated HCS/SCS sandstones; FA2-3: thin amalgamated HCS/SCS sandstones interbedded with thin mudstone beds	FA2-1 overlie FA1 and underlie FA3-FA6; FA2-2 overlie FA2-1 and FA2-3; FA2-3 is overlain by mixed- influence mouth bars and sandy deposits (FA4) or wave- or tide- influenced distributary-channel fill deposits (FA6)	FA2-1 represents the storm wave-dominated subaqueous delta; FA2-2 is located on the storm wave-dominated shoreline clinoform; FA2-3 represents deposits on the subaqueous platform
FA3: river mouth bars	Sandier- and coarsening- upward; 5–15 m thick	Thin, interbedded very fine-grained sandstones and siltstones/mudstones grading upwards to amalgamated sandstone beds; Soft-sediment-deformed beds; Sandstone are parallel-laminated to current-rippled, sometimes gradually change to unidirectional low-angle cross bedding; normally grading & structureless in sandstone layer; abundant plant debris/organic matter; No bioturbation	FA3 overlies the mixed-influenced mouth bars and sandy deposits (FA4) or sometimes is underlain by fluvial-influenced distributary-channel fill (FA5)	FA3 is located on the upper shoreline clinoform foreset
FA4: mixed-influence mouth bars& sandy deposits	Sandier- and coarsening- upward; 5–10 m thick	Parallel laminated to unidirectional current-rippled sandstones; wave ripples and bidirectional current ripples with occasional double mud drapes in the lower succession; HCS/SCS sandstone beds sharply overlying parallel-laminated sandstones of FA3; rare bioturbation (BI = 0–1) ( <i>Planolites</i> )	FA4 overlies thick coarsening-upward packages of FA1-1 & FA2-1, and is overlain by river mouth bar deposits (FA3); sometimes associated with FA6 in places	FA4 developed on the lower shoreline clinoform foreset to the subaqueous platform
FA5: fluvial-influenced distributary-channel fill deposits	Upward-fining or 'blocky' grain-size packages; 2–4 m thick	Unidirectional trough to low-angle cross bedded and parallel- laminated sandstones with mud rip-up clasts overlying erosional bases; Soft-sediment-deformed strata in places; No bioturbation	FA5-1 overlies thick, amalgamated HCS/SCS of FA2-1; F5-2 overlies amalgamated HCS strata (FA2-2); F5-3 overlies river-dominated mouth bars of FA3	FA5-1 developed on the outer subaqueous platform; FA5-2 developed on storm wave-dominated shoreline; FA5-3 located on the upper shoreline clinoform foreset
FA6: wave- or tide- influenced distributary-channel fill deposits	Upward-fining grain-size packages; 2–6 m thick	FA6-1: very sandy with unidirectional trough to low-angle cross bedded sandstones changing upward into HCS/SCS and wave-rippled sandstones; FA6-2: bidirectional cross beds above erosional bases gradually changing upward to heterolithic strata with bidirectional current ripples and/or double mud drapes along the ripple laminae	Some FA6-1 stacked above the thick coarsening-upward succession (FA1-1&FA2-1); Other FA6-1 and FA6-2 are associated with mixed-influence mouth bars and sandy deposits (FA4)	FA6-1 developed on the subaqueous platform FA6-2 and some FA6-1 developed on the lower shoreline clinoform foreset

associated with fluvial-dominated or wave-influenced channel deposits of FA5 and FA6 (e.g., 50 m in Fig. 2). Bioturbation in FA2-2 and FA2-3 is rare to absent (BI = 0–1).

**Interpretation.** This facies association, which was previously interpreted as wave-dominated delta front and shoreface (Peng et al., 2020b), is re-interpreted based on different stratigraphic locations and sedimentary characteristics. The coarsening- and thickening-upward successions (30–50 m thick) of FA2-1 (Figs. 2 and 3) are interpreted as storm-wave-dominated subaqueous delta. The lower portion of the succession, comprising interbedded mudstones and relatively thin beds of HCS/SCS sandstones, is interpreted as storm-wave-dominated subaqueous foreset deposits. Within these foresets, heterolithic strata with bioturbation are prevalent, suggesting a periodic sediment reworking and deposition. The normally graded beds associated with wave ripples are interpreted as products of wave-enhanced sediment-gravity flows on the foresets (Macquaker et al., 2010; Flint, 2014). The more intense

bioturbation of the heterolithic intervals at Radix Point suggests this part of the subaqueous clinothem was located further downstream and was less influenced by fluvial influence. The sandier, coarsening-upward units with thick, amalgamated HCS/SCS sandstones of FA2-2 are interpreted to represent storm wave-dominated shoreline clinothem (Figs. 2 and 3), analogous to other documented storm wave-dominated delta fronts or shorefaces (e.g., Hampson and Storms, 2003). FA2-3 is interpreted as deposits formed on a subaqueous platform, representing erosional and bypass zones predominantly influenced by waves. In areas where wave or storm wave energy diminishes, the platform can also aggrade, resulting in variable thickness across different locations (Fig. 2). The presence of amalgamated HCS/SCS or parallel-laminated sandstone beds with erosional surfaces and very rare bioturbation is due to the highly intense erosion, sediment reworking and redeposition by storm waves (Figs. 2 and 3). The depositional processes and associated facies on the subaqueous platform in this wave-dominated setting

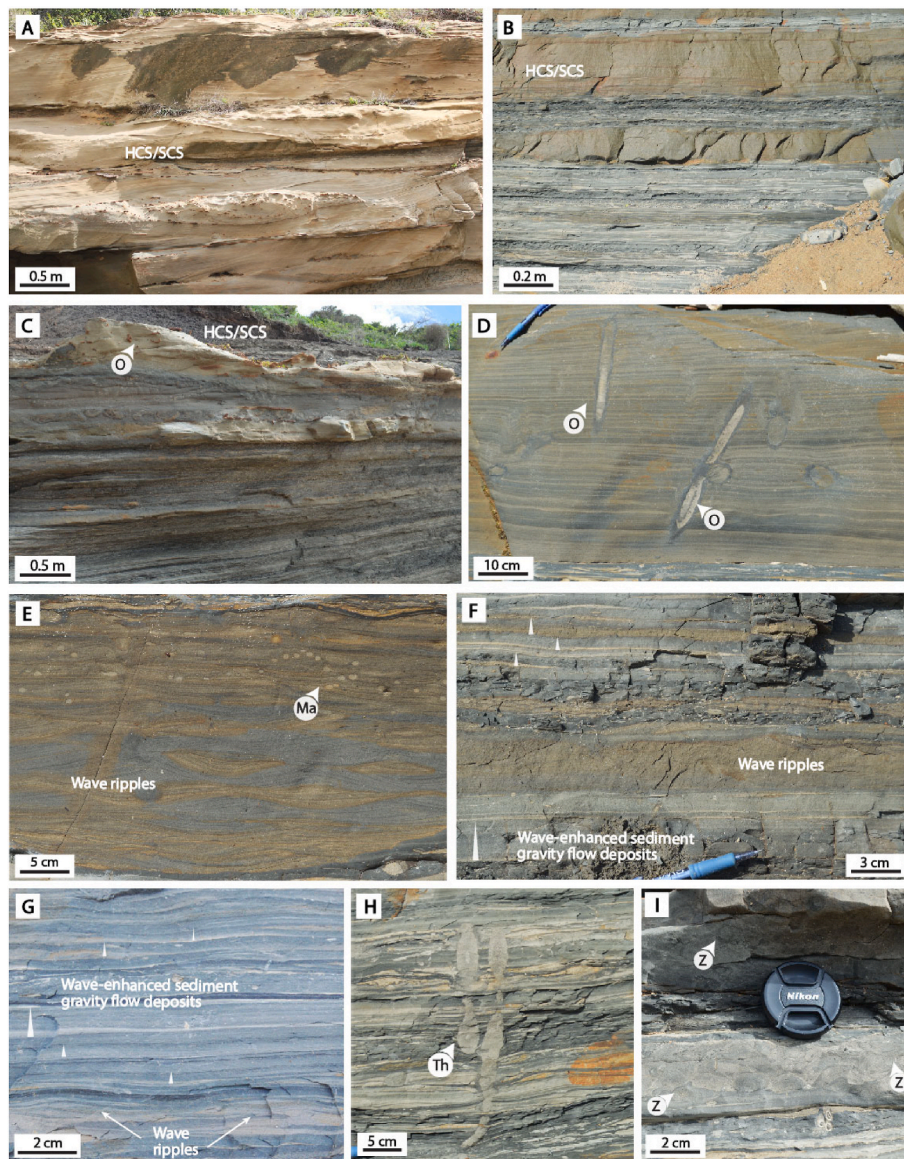


**Fig. 4.** Wave-dominated deposits of FA2 (A–E) and siltstones and mudstones with thin sandstone beds of FA1 (F–I). (A) Thick, amalgamated HCS/SCS sandstones. (B) A coarsening- and thickening-upward succession characterized by thin beds of HCS/SCS sandstones and muddy intervals. (C) Siltstones and mudstones interbedded with some thin HCS/SCS sandstone beds. (D) HCS/SCS beds with *Ophiomorpha* (O). (E) Wave-rippled sandstones. (F–G) Thin, normally graded beds interpreted as wave-enhanced sediment gravity flow deposits due to their associations with wave ripples. (H) Heterolithic beds with *Thalassinoides* (Th). (I) Siltstone beds that were thoroughly bioturbated with *Zoophycos* (Z). Photograph (A) is from Guayaguayare Bay; photographs (B–I) are from Radix Point.

differ from other platforms that are influenced by tides or other currents (Palamenghi et al., 2011; Cummings et al., 2015; Peng et al., 2018b; Osman et al., 2024; Steel et al., 2024).

#### 4.1.3. Facies association 3: river mouth bars

**Description.** FA3 is characterized by 5–15 m thick successions that become sandier and coarser upward, marked by interbedded very fine-grained sandstones and siltstones/mudstones that transition upward into amalgamated sandstone beds (Figs. 2 and 5A–C). Soft-sediment-deformed beds (0.1–0.7 m thick) of sandstones or interbedded sandstones and siltstones (Fig. 5B and C) frequently occur within the succession (210–270 m in Fig. 2). The sandstone beds commonly exhibit parallel-to current-rippled lamination (Fig. 5), which occasionally grades upwards to unidirectional low-angle cross bedding. Thin, normally graded sandstones and structureless sandstones (2–7 cm thick) are sometimes associated with abundant plant debris/organic matter. No bioturbation is observed. Stratigraphically, FA3 typically overlies the

mixed-influence mouth bars and sandy deposits of FA4 and sometimes is overlain by the fluvial-influenced channel fills of FA5 (e.g., channel 7) (Fig. 2).

**Interpretation.** The sandier- and coarsening-upward successions of FA3 are interpreted to represent river mouth bars (Ahmed et al., 2014; Ainsworth et al., 2016; Van Yperen et al., 2020). The frequent soft-sediment-deformed beds were likely due to rapid sediment loading of high river-derived sediment supply and over-steepening. The thin, normally graded sandstones and structureless sandstones associated with organic matter are interpreted as river-fed hyperpycnites (Mulder et al., 2003; Van Der Kolk et al., 2015; Jerrett et al., 2016; Zavala and Pan, 2018) that were deposited on the distal and proximal mouth bar deposits, respectively. The lack of bioturbation indicates a highly stressed environment (MacEachern et al., 2005; Dasgupta et al., 2016) which is consistent with the interpretation of river mouth bars (Peng et al., 2020b). Additionally, the stratigraphic positioning of FA3, situated beneath FA5 and above FA4, suggests that FA3 was likely deposited



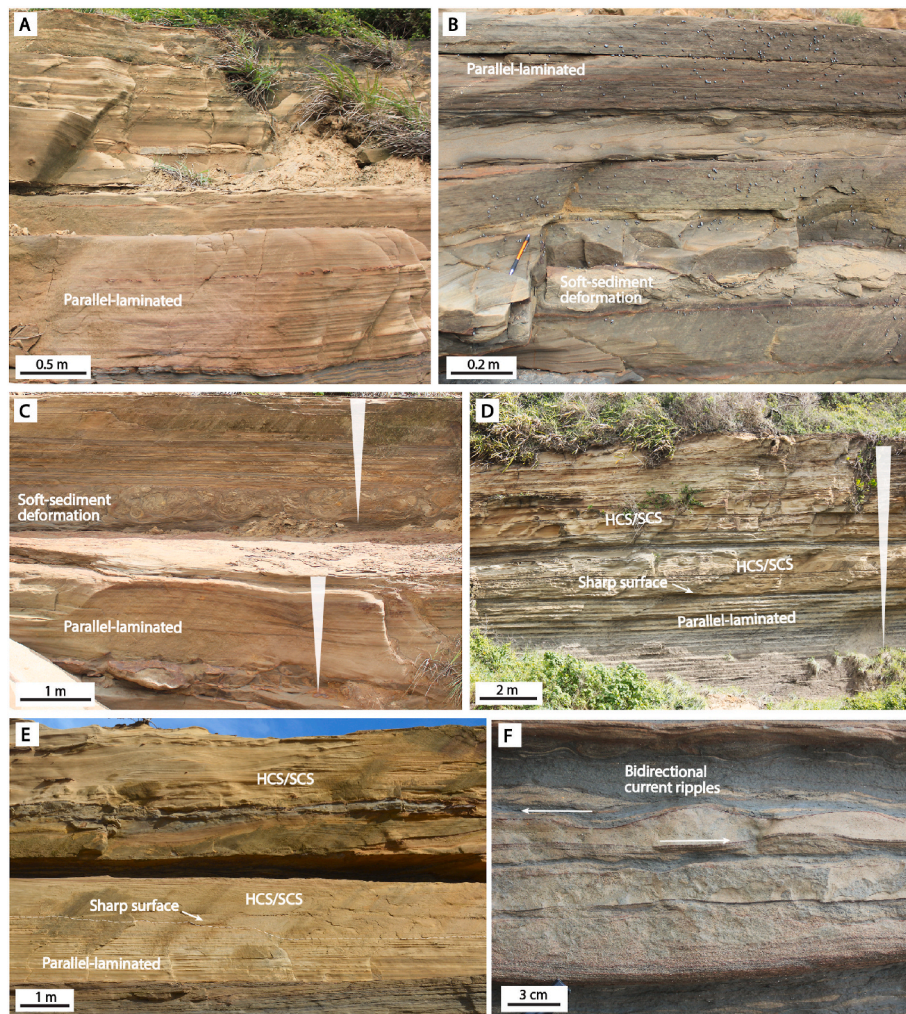


**Fig. 5.** Fluvial-dominated mouth bar deposits of FA3 (A–C) and mixed-influenced mouth bar and sandy bar deposits of FA4 (D–F). (A) Parallel-laminated sandstones with thin siltstones. (B) Parallel-laminated sandstone and siltstone beds with soft-sediment deformation. (C) Two coarsening-upward units of heterolithic beds changing upwards to parallel-laminated sandstones with a soft-sediment-deformed bed. (D) A coarsening- and sandier-upward succession of unreworked, interbedded parallel-laminated sandstones and siltstones in the lower part, and HCS/SCS sandstones as reworked upper part. (E) The uppermost part of mouth bar deposits showing parallel-laminated sandstones overlain by HCS/SCS sandstones. (F) Bidirectional ripples preserved in some heterolithic intervals. Photographs (A–F) are from Guayaguayare Bay.

in a proximal setting, such as the upper shoreline/delta-front clinoform foresets. This setting was situated basinwards of fluvial distributary channels, but landwards from significant marine reworking processes.

#### 4.1.4. Facies association 4: mixed-influence mouth bars and sandy deposits

**Description.** FA4 has the same coarsening- and sandier-upward trend with parallel bedding to unidirectional current-rippled sandstones as in FA3. However, it contains wave ripples and bidirectional current ripples, indicating paleoflow directed towards the southeast and northwest (Fig. 5D–F). Occasionally, double mud drapes are observed in the lower parts of some successions. The upper portion of FA4 exhibits HCS/SCS sandstone beds sharply overlying parallel-laminated sandstones (0.5–1.5 m thick) (Fig. 5D and E). The proportion of strata characterized by these sedimentary structures accounts for 50 %–70 % of the total strata in FA4. Bioturbation is sparse (BI = 0–1) with occurrence of *Planolites* (P) in some muddy beds. FA4 commonly occurs stratigraphically above thick coarsening-upward packages of FA1-1 and FA2-1, and is overlain by the fluvial mouth bar deposits (FA3) (Fig. 2). In places, such as 117–137 m in the measured section, they are associated with wave- or tide-influenced channel fill deposits of FA6.

**Interpretation.** The wave ripples and bidirectional current ripples with occasional double mud drapes in the lower succession indicate that

distal mouth bars were reworked by storm waves and tidal currents. The parallel-laminated to HCS/SCS sandstone beds in the upper portion of FA4 suggest that the upper/proximal part of the mouth bars were reworked by storm waves intermittently. This facies association was previously interpreted as mixed-process shoreline-attached delta front (Peng et al., 2020b). However, its relative stratigraphic position suggests that they were likely located basinwards of river mouth bars probably on the lower shoreline clinoform foreset and subaqueous platform that was reworked by wave and tidal processes.

#### 4.1.5. Facies association 5: fluvial-influenced distributary-channel fill deposits

**Description.** FA5 is characterized by upward-fining or ‘blocky’ grain-size packages (2–4 m thick) (Fig. 2) of unidirectional trough to low-angle cross bedded and parallel-laminated sandstones with mud rip-up clasts overlying erosional bases (Fig. 6A, C, D). Soft-sediment-deformed strata (i.e., convolute bedding) occur at their bases in places. No bioturbation is observed in these distributary-channel fills. FA5 can be further delineated into FA5-1, FA5-2 and FA5-3 based on their grain sizes and varying stratigraphic positions. The sediment comprising the distributary channel fills of FA5-1 is predominantly lower very fine-grained, whereas the grain sizes of FA5-2 and FA5-3 range from upper very



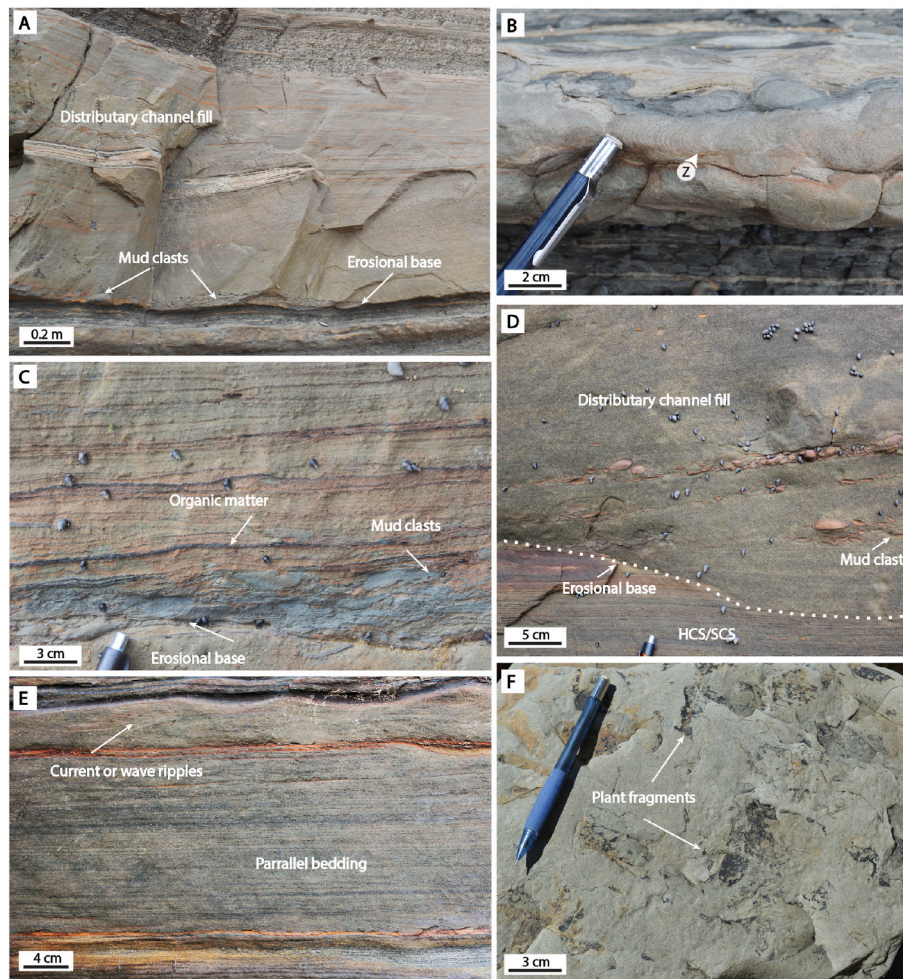


**Fig. 6.** Fluvial-influenced distributary-channel fill facies associations. (A) A thin, sandy distributary-channel fill with mud clasts overlying the erosional base. (B) A siltstone layers showing well developed *Zoophycos* (Z). (C–D) An erosional-based sandstone unit with abundant mud clasts. (E) Parallel-laminated sandstones and overlying current ripples in distributary-channel fills. (F) Plant fragments on the surface of silty mudstones. Photographs (A–F) are from Guayaguayare Bay.

fine- to lower fine-grained. Relatively thin FA5-1 channels (1–1.5 m thick), such as channel 1, truncated down into upward-coarsening heterolithic units characterized by abundant wave ripples and some HCS strata (FA1-1 and FA2-1). FA5-2 channels (2–4 m thick), such as channels 2 and 3, overlie the amalgamated HCS/SCS strata (FA2-2). FA5-3 channels (e.g., channel 7) are located above fluvial-dominated mouth bars (FA3) (Fig. 2).

**Interpretation.** The upward-fining or ‘blocky’ grain-size packages of unidirectional trough to low-angle cross bedded and parallel-laminated sandstones are interpreted as fluvial-influenced distributary-channel fills (Olariu and Bhattacharya, 2006; Lin et al., 2020; Peng et al., 2020b). The mud rip-up clasts and erosional bases indicate the relatively high energy of currents. The relatively finer grain size of FA5-1 compared to FA5-2 and FA5-3 suggests that FA5-1 channels were likely located more basinward. The FA5-1 channels (e.g., channel 1, Fig. 2) are interpreted as distributary-channel fills developed on the subaqueous platform which sharply overlie the upward-coarsening heterolithic units of the subaqueous delta (FA1-1 and FA2-1). Alternatively, FA5-1 channels can be storm-surge deposits formed when large storm waves travelled back in the offshore direction (Amos et al., 2003; Gallop et al., 2011; Castelle and Coco, 2012). FA5-2 channels (e.g., channels 2, 3 in Fig. 2) that overlie the amalgamated HCS/SCS strata (FA2-2) are interpreted to represent distributary-channel fills truncating down the storm wave-dominated shoreline clinothem. FA5-3 channels (e.g., channel 7, Fig. 2) overlying the fluvial-dominated mouth bars (FA3) are interpreted as distributary-channel fills on the upper shoreline clinoform foreset

where there was more river-derived sediment supply (Peng et al., 2020b).

#### 4.1.6. Facies association 6: wave- or tide-influenced distributary-channel fill deposits

**Description.** FA6 is characterized by a general fining-upward package (2–6 m thick) overlying an erosional base with mud rip-up clasts (Fig. 7). Two types of FA6 were identified in the measured section. FA6-1 channels (e.g., channels 4, 5, 8, 11, 12) contain unidirectional trough to low-angle cross bedded sandstones changing upward into HCS/SCS and wave-rippled sandstone beds (Fig. 2). Some of these channels (e.g., channel 11) overlie the relatively muddy, coarsening- and thickening-upward succession (FA1-1 and FA2-1) (Fig. 2). FA6-2 channels (e.g., channel 9 and 10) predominately consist of bidirectional cross beds (towards the southeast and northwest) gradually changing upward to heterolithic strata with bidirectional current ripples and/or double mud drapes along the ripple laminae (Fig. 7C). Occasionally some HCS/SCS beds, wave ripples and unidirectional current ripples are observed in the distributary-channel fills. Other FA6-1 channels (e.g., channel 8) and FA6-2 channels are stratigraphically associated with mixed-influence mouth bars and sandy deposits of FA4 (Fig. 2).

**Interpretation.** The unidirectional trough to low-angle cross bedded sandstones grading upward into HCS/SCS and wave-rippled sandstone beds suggest that wave processes winnowed finer sediments and particularly reworked or interacted with the upper part of the FA6-1 channel infills. The FA6-1 channels, which overlie the muddy



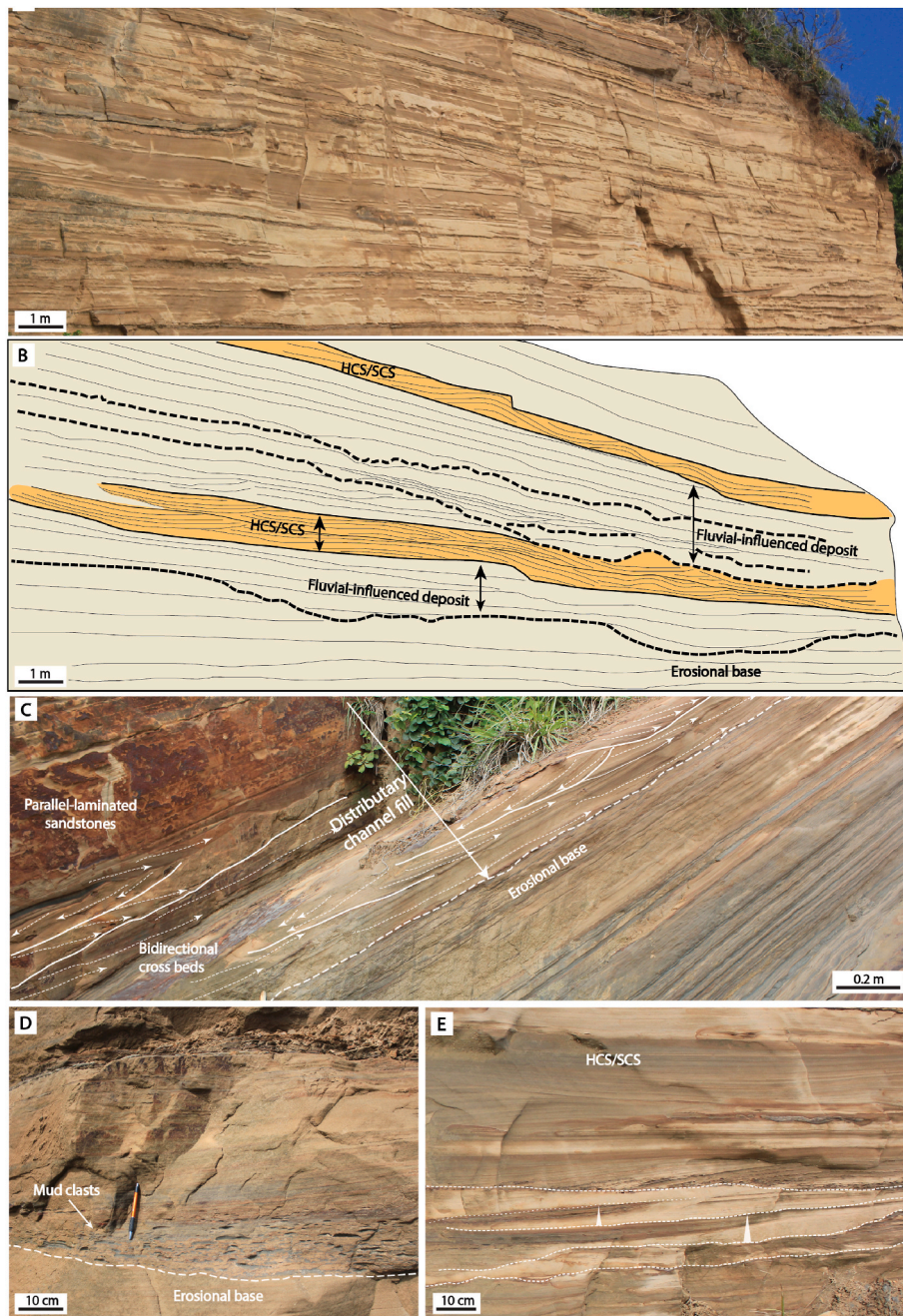


**Fig. 7.** Mixed-influence distributary-channel fill facies associations. (A–B) Stacked distributary-channel fills with fluvial deposits in the lower part and wave-reworked deposits, such as HCS/SCS beds in the upper part. (C) A distributary-channel fill showing bidirectional cross beds on the bottom and overlying parallel-laminated sandstones. (D) An erosional-based, parallel-laminated sandstones with abundant mud clasts in one mixed-influence distributary-channel fill. (E) A distributary-channel fill showing multiple erosional-based fining-upward units in the lower part and HCS/SCS sandstones in the upper part. Photographs (A–E) are from Guayaquayare Bay.

coarsening-upward successions (FA1-1 and FA2-2), are interpreted as wave-influenced channels developed on the lower shoreline clinoform foreset or subaqueous platform. Intense wave actions facilitated scouring on the subaqueous platform, resulting in the formation of channels in front of delta flanks and inter-deltaic areas. This process occurred as longshore currents returned offshore or as longshore drifts converged, subsequently redirecting offshore within the inter-deltaic areas (Willis et al., 2021). The FA6-2 channelized units, characterized by bidirectional cross beds together with bidirectional current ripples and double mud drapes, are interpreted as tide-influenced distributary-channel fills. The HCS/SCS beds, wave ripples and unidirectional current ripples indicate waves and fluvial currents also had some minor influence in the

FA6-2 distributary-channel fills. The FA6-1s and FA6-2s that are stratigraphically associated with mixed-influence mouth bars and sandy deposits (FA4) are interpreted to represent wave- and tide-influenced distributary-channel fills developed on the lower parts of the shoreline clinoform foresets.

#### 4.2. Reconstruction of the Moruga compound clinoform

The uppermost two sub-wedges of the Moruga Formation represent two main forward-stepping deltas bounded by major flooding surfaces (Fig. 8). These flooding surfaces occur at the top of coarsening-upward units of shoreline clinoforms. A major flooding surface is identified at



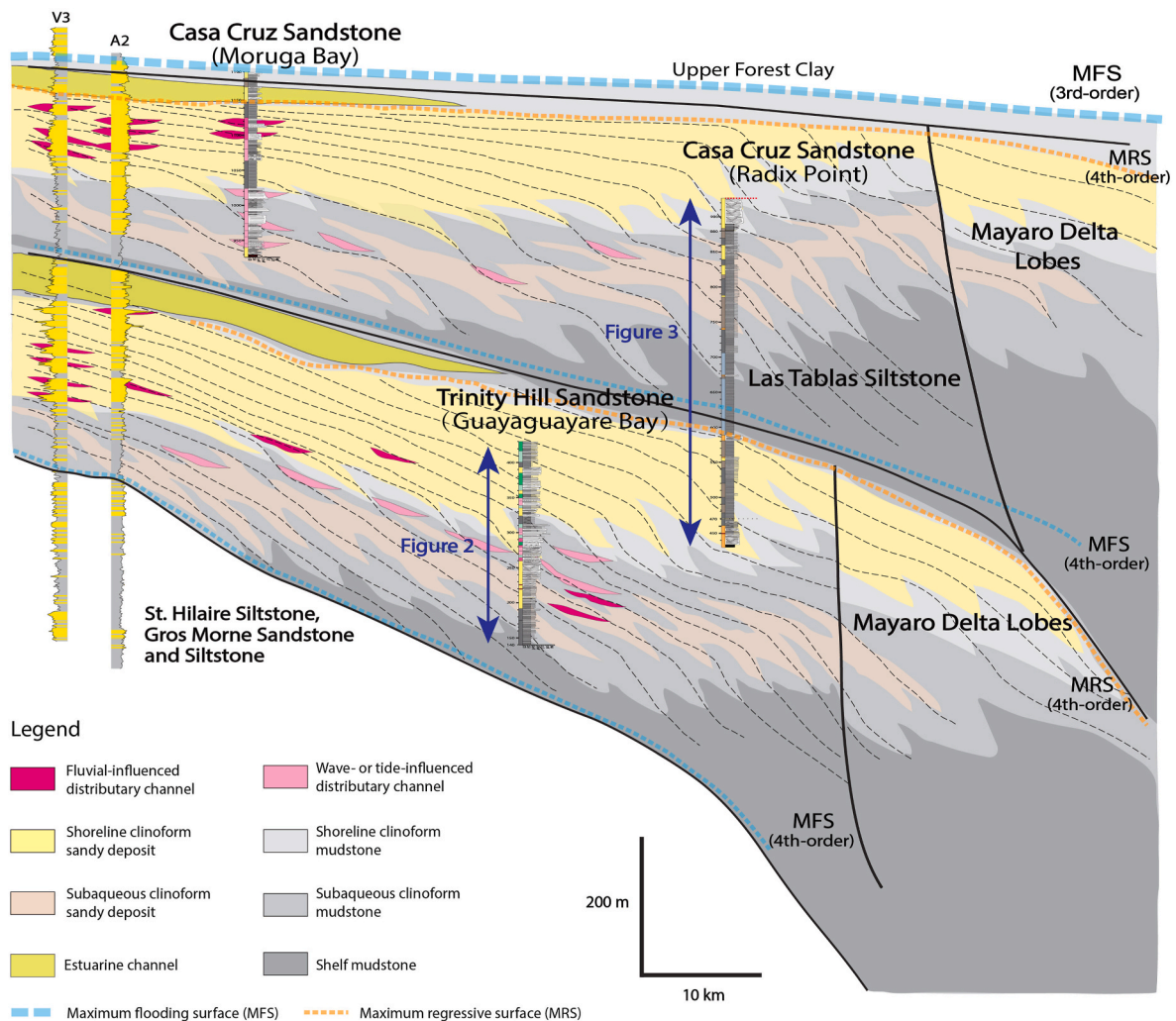


**Fig. 8.** Reconstruction of the compound clinoform delta in the Trinity Hill Sandstone and the Las Tablas Siltstone-Casa Cruz Sandstone deltaic clastic wedges. Wells V3 and A2 to the left are from [Chen et al. \(2017\)](#). The three measured sections were documented by [Peng et al. \(2020b\)](#).

the boundary between the Trinity Hill Sandstone and Las Tablas Siltstone members (i.e., 160 m in [Fig. 3](#)). Overlying this surface are thick shelf mudstones and muddier deposits of subaqueous clinoforms ([Figs. 2 and 3](#)). The sub-wedge is characterized by deposition of progradational compound clinoforms. These sub-wedges developed within a highly subsiding shelf margin, evidenced by high sediment accumulation rates ( $>1$  km/My; [Wood, 2000](#); [Chen et al., 2017](#)) and by the relatively high angle of the rising shelf-edge trajectory judged from the seismic data ([Peng et al., 2020b](#)). Consequently, we suggest that this aggradational nature of the shelf margin likely facilitated preservation of the compound-clinoform delta.

The Trinity Hill Sandstone Member contains strata dominated by stacked shoreline clinoforms ([Figs. 2 and 8](#)), each ranging in thickness from 5 to 15 m. At Guayaguayare Bay, the strata were deposited by actively building deltaic lobes situated close to the distributary channels of the main sediment source, which is supported by the frequent presence of fluvial-dominated to mixed-process-influenced mouth bars and distributary-channel fills ([Figs. 5–7](#)). Shoreline clinoforms are dominated by a variety of process regimes ([Fig. 2](#)). At levels 57–90 m in [Fig. 2](#), the shoreline clinoforms are storm wave-dominated with occasional fluvial-influenced channels in the uppermost part. The shoreline clinoforms at level 98–137 m contain channel and mouth-bar deposits that were influenced by an interplay of fluvial, wave, and tidal processes (also see [Section 5.2](#)). The two sets of shoreline clinoforms in 175–270 m ([Fig. 2](#)) are dominated by fluvial and wave processes. The Casa Cruz

Sandstone Member (470–500 m in [Fig. 3](#)) exhibits storm wave-dominated shoreline clinoforms probably due to great distance from river input at Radix Point.

Muddy successions in the Trinity Hill Sandstone ([Fig. 2](#)) and in Las Tablas Siltstone members ([Fig. 3](#)) were interpreted as subaqueous-delta clinoforms characterized by multiple stacks of 30–50 m thick, mud-prone coarsening-upward successions ([Fig. 8](#)). The successions comprise heterolithic intervals with relatively thin HCS/SCS beds eventually passing upwards to amalgamated HCS/SCS beds, indicating an increase in storm wave energy as water depth decreased. The subaqueous platform, located stratigraphically between the shoreline clinoforms and subaqueous clinoforms, contains deposits produced by wave, tidal or fluvial processes (also see [Section 5.1](#)). At Guayaguayare Bay, the subaqueous clinoform in the Trinity Hill Sandstone Member is sand-prone ([Fig. 2](#)) probably due to proximity to river mouths in its upstream reach. The Las Tablas Siltstone Member at Radix Point is very muddy ([Fig. 3](#)), but with abundant thin ‘event’ beds formed by wave-enhanced sediment gravity flows ([Fig. 4F and G](#)) and are interpreted to represent the Las Tablas subaqueous clinoform in its downstream reaches. This lateral distribution of proximal and distal segments of the subaqueous clinoform is supported by numerous modern delta examples, which exhibit skewed subaqueous clinoforms that align parallel to the coast in offshore wave- and current-dominated settings ([Tesson et al., 2000](#); [Cattaneo et al., 2003](#); [Neill and Allison, 2005](#)).

## 5. Discussions

### 5.1. How various types of channelized flow drive compound-clinoform deltas

Wave-dominated deltas typically exhibit fewer distributary channels because waves often remobilize river mouth bars (Geleynse et al., 2011; Nardin and Fagherazzi, 2012; Nardin et al., 2013), resulting in less frequent avulsion than in river-dominated deltas (Jerolmack and Swenson, 2007). However, no ancient examples illustrating channel dynamics in these wave-dominated delta settings have been documented. In the Moruga Formation, which was interpreted as a wave-dominated delta (Peng et al., 2017, 2020b), various channel types have been preserved, constructed through dynamic interactions of fluvial, tidal and wave processes. The preservation of these distinct channel types further indicates lateral variation in process regimes within the deltaic lobes.

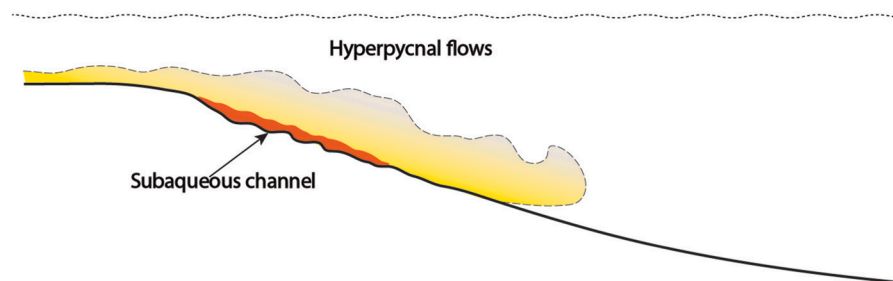
In some parts of the lower foreset/delta front of shoreline clinoforms, channels exhibit stronger tidal influence than wave influence (i.e., channels 9 and 10 in Fig. 2). These tide-influenced channels were likely located in embayments that may have developed as coastline irregularity/roughness increased, potentially leading to tidal amplification (Anell et al., 2021). The muddy feature of channel 9 (Fig. 2) also suggests the possible presence of embayments or restricted bays that may have been partially protected from open-marine waves. Alternatively, the preserved tide-influenced channels may have developed in zones characterized by sheltered coastal morphology (Peng et al., 2020b) or structural constriction (Anell et al., 2021). In the measured section, the tide-dominated channels are less frequent, suggesting that tidal influence was subsidiary to wave influence in the study area.

Significant fluvial and wave influence on channels across most shoreline clinoforms and subaqueous platforms indicates that fluvial and wave processes played an important role in channel dynamics and in the delta-building processes. Wave influence tended to increase as the

subaqueous channels progressively migrated basinwards or laterally (Willis, 2005; Pontén and Plink-Björklund, 2007; Van Cappelle et al., 2016; Collins et al., 2018). At Guayaguayare Bay in a setting closer to the river sediment supply, fluvial- and wave-influenced subaqueous channels (i.e., channels 4, 11 and 12) (Fig. 2) were well developed on the shoreline clinoform and subaqueous platform. The preserved strata at the base of the channels (FA6-1) are mainly fluvial-influenced deposits, whereas the upper distributary-channel fills show HCS/SCS strata with few tidal signals (i.e., bidirectional asymmetrical ripples). The HCS/SCS strata within the upper distributary-channel fills not only indicate intense reworking of river-derived deposits but also capture and preserve the strong interaction between waves and river floods. This interaction likely provided wave-turbulence buoyancy to the hyperpycnal flows, allowing them to travel much farther across the platform (Fig. 9). The wave-induced suspension of riverine hyperpycnal flows is supported both by the analytical model (Friedrichs and Wright, 2004) and modern examples (e.g., Mitchell et al., 2012). Similar subaqueous hyperpycnal channels formed through cut and fill processes generated by storms and/or river floods have been documented in wave-dominated deltaic deposits within the Aberdeen Member at Book Cliffs in eastern Utah (Pattison et al., 2007). The frequent presence of wave-influenced channels on the subaqueous platform and lower shoreline clinoform (Fig. 2) may suggest somewhat more frequent bifurcation and avulsion of channels across the wave-scoured substrate compared to subaerial wave-influenced distributary channels (Willis et al., 2021).

Fluvial-influenced channels (FA5) and their associated underlying river mouth bars (FA3) developed mainly on the upper shoreline clinoform foreset (i.e., channels 2, 3, 6, 7). In places, fluvial-influenced channels are also observed on the subaqueous platform (i.e., channel 1). This indicates that some channels with a high flood supply of river-derived sediment from the distributary channels could have penetrated further basinward onto the subaqueous platform (Fig. 10).

(A) Fluvial-influenced distributary channels



(B) Fluvial- & wave-influenced distributary channels

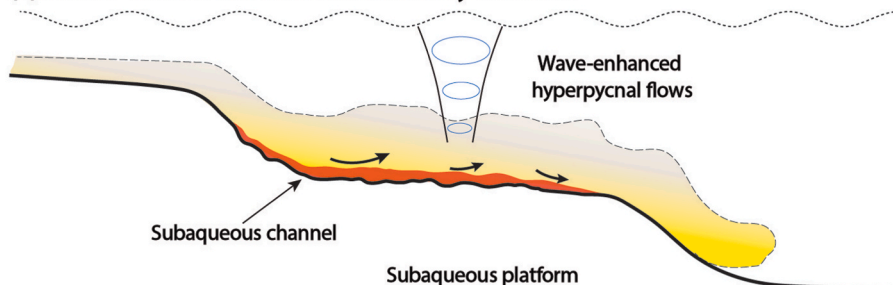


**Fig. 9.** Schematic diagram showing comparison of hyperpycnal flows in fluvial-influenced subaqueous distributary channels (A) and in fluvial- and wave-influenced distributary channels (B). Note that waves provide turbulent support for hyperpycnal river floods causing the subaqueous channels to extend farther across the subaqueous platform.

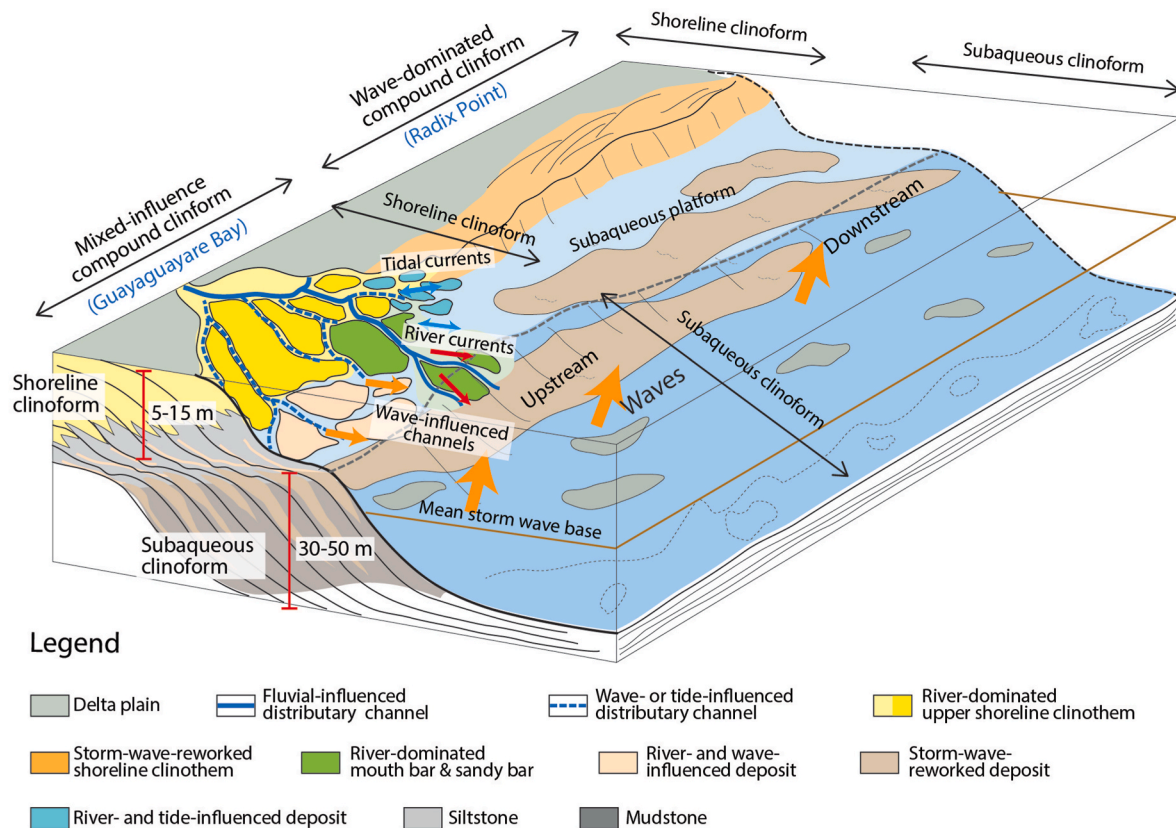


**Fig. 10.** Schematic three-dimensional block diagram of mixed-influence compound clinoform in the upstream (Guayaguayare Bay) and wave-dominated compound clinoform delta in the downstream (Radix Point).

## 5.2. How fluvial, tidal, and wave processes interacted on the compound clinoform

**Wave Signals:** Waves produce the dominant signal in the subaqueous clinothem, the subaqueous platform and some shoreline clinothem of the Moruga Formation. Wave signals generally increase from the bottomset up through the foreset of subaqueous delta. The relatively thin HCS/SCS beds in the lower subaqueous foreset (FA2-1) indicate that deposits in this zone were only periodically emplaced or influenced by larger storm waves. Some regions of the subaqueous platform were primarily impacted by storm waves, particularly within abandoned deltaic lobes where fluvial and tidal influences is much less pronounced (e.g., 52–58 m in Fig. 2). In these areas, storm waves penetrated landwards and upwards to the shoreline bottomset, resulting in the formation of gutter casts filled by HCS/SCS beds within the muddy successions (e.g., 232–240 m in Fig. 2). On the lower part of the shoreline clinoform and subaqueous platform, particularly in areas affected by significant river discharge, the offshore back surges of storm waves likely provided turbulent support for the river-derived hyperpycnal/hypopycnal flows (Myrow and Southard, 1996; Bentley, 2003; Wright and Friedrichs, 2006; Macquaker et al., 2010). This may have facilitated the connection and maintenance of subaqueous channels from the shoreline clinoform toward the subaqueous rollover, consequently enabling further offshore sediment transport (Fig. 9). This process is evidenced by the well-developed wave-enhanced sediment gravity flow deposits (FA2-1) that formed in the upper foreset of the subaqueous delta (Fig. 3) during abrupt increases in deposition rate (Peng et al., 2020a). These gravity flows became finer grained and thinner downslope as they waned onto the bottomsets. Shoreline clinothem (e.g., 58–80 m in Fig. 2) display significant and frequent storm wave influence, as evidenced by the amalgamation of HCS/SCS sandstones into relatively thick beds (FA2-2) (cf., Dumas and Arnott, 2006).

**Fluvial Signals:** Fluvial processes are primarily evident on the shoreline clinoform and on the proximal-mid reaches of the subaqueous platform, as indicated by abundant fluvial hyperpycnites with organic matter/plant debris, lack of bioturbation, and frequent soft-sediment-deformed beds (FA3 and FA 5) (Peng et al., 2018a). The fluvial signals generally increase upward within each foreset of the shoreline clinoform at the parasequence scale (e.g., 117–126 m or 132–138 m), as particularly illustrated from 107 to 137 m in Fig. 2. Each parasequence is characterized by well-developed fluvial-dominated and mixed-influence channels and mouth bars. Relatively high sediment supply and rapid subsidence rates contributed to the effective preservation of fluvial signals within the predominantly wave-dominated environment of the Moruga Formation (Peng et al., 2020b).

**Tidal Signals:** Tidal processes are evident in some distributary-channel fills (FA6-2) and mixed-influence mouth-bar and sandy deposits (FA4) that developed on the lower foreset/delta front of the shoreline clinoform and on the subaqueous platform. In places, the bottom of some distributary-channel fills (e.g., channels 9 and 10) (Fig. 2) are characterized by bidirectional cross-bedded sandstones (towards the southeast and northwest) that are interpreted as tidal-bar deposits (Fig. 7C). Some relatively muddy channels (e.g., channel 9) and the lower parts of mixed-influence mouth bars show bidirectional current ripples (Fig. 5F), double mud drapes and fluid muds, suggesting they were strongly influenced by tidal processes. Process histogram at 117–137 m in Fig. 2 shows more obvious tidal influences particularly on the lower parts of the shoreline clinoform at the parasequence scale (Fig. 2). These muddy and organic-matter-rich units with well-preserved tidal signals were interpreted to represent tidal deposits that developed in the inter-deltaic embayment areas (Fig. 10). In forward models of wave-dominated, compound-clinoform deltaic environment, the inter-deltaic deposits tended to extend nearly as far as the axial deltaic deposits due to the strong littoral drift of waves (Willis et al., 2021). As



such, the tide-influenced inter-deltaic deposits would likely become commonly juxtaposed vertically with the axial river- and wave-dominated deltaic deposits.

The two compound-clinoform successions also exhibit a general shift in process regime over time (Fig. 2). Both successions (i.e., 0–137 m and 137–270 m) consist of several shoreline clinoforms and subaqueous platforms stacked above the subaqueous clinoforms. Processes on the subaqueous clinoforms are generally similar, characterized dominantly by storm wave processes with occasional fluvial and tidal influences on some subaqueous foresets. The shoreline clinoforms in the older succession are wave-dominated in the lower part, and they changed to systems influenced by a mixture of fluvial, wave, and tidal processes in the upper part (Fig. 2). In the younger succession, more river- and wave-dominated mouth bar deposits and fewer channels were developed, probably caused by changing dominant process regimes over time possibly due to autogenic processes or changes in sediment supply. The abundance of soft sediment deformations in these deposits suggests an increase in river-derived sediment supply, leading to destabilization of deposition on the shoreline clinoform foreset. The fluvial- and wave-domination in the younger succession could also have resulted from a narrower platform which led to less dampening of waves (Fig. 10) (Anell et al., 2021). The vertical juxtaposition of these successions could also suggest a dynamic deltaic environment characterized by lateral changing of process regimes along-strike. Such mixed-process deltaic systems with spatial process variations are common in both modern systems (Ainsworth et al., 2011; Nanson et al., 2013) and ancient records (Ainsworth et al., 2016; Rossi and Steel, 2016; Collins et al., 2018; Zhang et al., 2019).

### 5.3. Vertical discontinuity between the shoreline and subaqueous clinothem

Vertical discontinuity can be observed between the shoreline and subaqueous clinoforms. The Moruga succession in this study exhibits regressive units with a bi-partite character, showing an abrupt shift in grain size and facies. The upper sandy coarsening-upward units (5–15 m thick) are generally coarser in grain size (i.e., upper very fine- to lower fine-grained) and represent the shallow shoreline/delta-front clinoforms dominated by storm waves or influenced by mixed fluvial, wave and tidal processes (Fig. 2). The storm wave-dominated shoreline clinoforms are characterized by mudstones interbedded with HCS/SCS sandstones grading upward to thick amalgamated HCS/SCS sandstones (FA2-2). The mixed-influence shoreline clinoforms consist of fluvial-influenced channel and mouth-bar deposits (FA5 and FA3) in the upper portions, and mixed-influence channel and mouth bar deposits (FA6 and FA4) in the lower portions. The muddy coarsening-upward units (30–50 m thick) below each of the shoreline clinoforms are interpreted to represent the subaqueous clinoforms building gradually into slightly deeper water, but still on the shallow shelf, exhibiting a general upward increase in wave influence (Fig. 2). The extent of subaqueous clinoform development and depth of the subaqueous rollover are determined by a combination of factors including sediment supply, the intensity of the waves and currents (Pirmez et al., 1998) and also the platform width as wider platforms generally roll over in slightly deeper water. The Holocene Adriatic subaqueous clinoform, which was built by waves and shelf currents, exhibits similar thickness (i.e., approximately 35 m) with its subaqueous rollover located at a water depth of 30 m (Cattaneo et al., 2003, 2007; Pellegrini et al., 2015; Amorosi et al., 2016). The subaqueous platform, which connects the shoreline and subaqueous clinoforms, is influenced by fluvial processes proximally as well as waves, tides and other oceanic currents in the distal setting. The nature of mixed processes occurring on the subaqueous platform is governed by spatial and temporal variation in sediment supply, relative sea level, as well as basin and shoreline morphology. In areas strongly influenced by waves, the development of wave-scoured distributary-channel fills on the subaqueous platform can create vertical

separation between the shoreline and subaqueous clinoforms (Willis et al., 2021).

Process changes in the shoreline clinothem are more frequent than those in the subaqueous clinothem. In the regressive units of the Moruga Formation, there are more units of shoreline clinoforms than subaqueous clinoforms, though there are no 'distal' outcrops of these successions (Fig. 2). The multiple stacked shoreline clinoforms suggest a strong aggradation of shoreline clinoforms with variable process changes. The relative development of shoreline and subaqueous clinoforms depends on the interplay of fluvial sediment supply and basinal processes (Pirmez et al., 1998; Swenson et al., 2005; Walsh and Nittrouer, 2009). Additionally, shoreline clinoforms are more likely controlled by high-frequency allogenic and autogenic forcing, and therefore they tend to exhibit rapid episodes of progradation, abandonment, erosion and retreat (Cattaneo et al., 2003; Correggiari et al., 2005; Patruno et al., 2015). By contrast, subaqueous clinoforms are mainly controlled by hydrodynamic forces of waves or oceanic currents, which disperse sediment laterally and fill significantly larger and deeper spaces (e.g., modern Adriatic subaqueous delta; Cattaneo et al., 2003, 2007). Consequently, the subaqueous clinoform is constructed slowly through the consistent depositional processes of waves or currents across the shelf. Modelling results of Willis et al. (2021) additionally demonstrate that the shoreline clinoform tended to be eroded back after its abandonment and then prograded basinwards and expanded laterally, whereas the subaqueous clinoform continued to slowly prograde in the wave-dominated, compound-clinoform delta.

## 6. Conclusions

The studied Moruga Formation of the paleo-Orinoco Delta is interpreted to represent a compound-clinoform delta with distinct upstream segment outcrops at Guayaquayare Bay and a downstream segment at Radix Point. This deltaic system comprises multiple stacked shoreline and subaqueous clinoforms mainly influenced by fluvial and wave processes. Notably, both the shoreline and subaqueous clinoforms exhibit a coarsening-upward trend, characterized by distinct vertical and spatial variations in grain size, thickness and facies. The shoreline clinothem is typically coarser grained and ranges from 5 to 15 m in thickness. In contrast, the subaqueous clinothem is muddier and exhibits thicknesses ranging from 30 to 50 m.

The shoreline clinoforms are wave-dominated and mixed-influence in their upstream reaches, whereas they are wave-dominated in the downstream reaches. The wave-dominated shoreline clinoforms consist of amalgamated HCS/SCS sandstones interbedded with siltstones/mudstones grading upward to thick amalgamated HCS/SCS sandstones. The mixed-influence shoreline clinoforms are composed mainly of fluvial-influenced channels, mouth bars and shorefaces on the upper foresets, and mixed-influence mouth bars and channels on the lower foresets to bottomsets.

The subaqueous clinoforms are muddier, characterized by interbedded siltstones/mudstones and HCS/SCS beds grading upwards to relatively thin amalgamated HCS/SCS beds, indicating a general upward increase in storm-wave influence. The subaqueous clinoform in the upstream area is sand-prone and predominantly influenced by fluvial and wave processes. In this region, some channels with strong river supply extended from the shoreline clinoform to the subaqueous platform. The subaqueous clinoform in the downstream area is dominated by storm wave processes, characterized by muddy successions with abundant relatively thin HCS/SCS or wave-rippled beds and wave-enhanced sediment-gravity-flow deposits. The subaqueous bottomsets are composed of thick siltstones and mudstones that exhibit moderate to high bioturbation.

The subaqueous platform is the transition interval between the shoreline and subaqueous clinothem and represents zones dominated by erosion, reworking and bypass processes. In the studied areas, the subaqueous platform is influenced by fluvial processes in the proximal

reaches and wave, tides and other oceanic currents in the distal reaches. In places where the subaqueous platform is closer to the river sediment supply, it exhibits mixed-influence subaqueous channels and sandy bars strongly affected by storm waves. The presence of wave- and fluvial-influenced channels on the subaqueous platform leads to a distinct vertical boundary between the shoreline and subaqueous clinothems. The wave-influenced channels and sandy bar deposits indicate that storm waves interacted with river floods in the subaqueous channels to provide buoyancy for the hyperpynal flows, causing significant extension of channels and sediment dispersal across the platform.

## CRedit authorship contribution statement

**Yang Peng:** Writing – original draft. **Ronald J. Steel:** Writing – review & editing. **Cornel Olariu:** Writing – review & editing. **Shunli Li:** Writing – review & editing.

## Declaration of competing interest

The authors declare that they have no known competing financial interests or personal relationships that could have appeared to influence the work reported in this paper.

## Acknowledgements

We thank RioMAR consortium sponsors (BHP Billiton, Chevron, Devon, Eni, ExxonMobil, Petrom, Shell, Statoil, Wintershall, and Woodside) and the University of Texas at Austin for their financial support of this work. YP acknowledges financial supports from the National Natural Science Foundation of China (No. 42202107) and the Science Foundation of China University of Petroleum, Beijing (No. 2462021BJRC002). Acknowledgments are extended to Clarke A. Clayton, Cory Hughes, Georgia Huggins, and Ariana Osman for their invaluable field assistance and local support on Trinidad. The authors are grateful to the reviewers Ingrid Anell, Alessandro Amorosi, and two anonymous reviewers for providing constructive comments that improved the quality of this manuscript and Stefano Patruno for handling the manuscript.

## Data availability

The data that has been used is confidential.

## References

- Ahmed, S., Bhattacharya, J.P., Garza, D.E., Li, Y., 2014. Facies architecture and stratigraphic evolution of a river-dominated Delta front, Turonian ferron sandstone, Utah, U.S.A. *J. Sediment. Res.* 84, 97–121. <https://doi.org/10.2110/jsr.2014.6>.
- Ainsworth, B.R., Vakarelov, B.K., MacEachern, J.A., Nanson, R.A., Lane, T.I., Rarity, F., Dashtgard, S.E., 2016. Process-driven architectural variability in mouth-bar deposits: a case study from a mixed-process mouth-bar complex, drumheller, Alberta, Canada. *J. Sediment. Res.* 86, 512–541. <https://doi.org/10.2110/jsr.2016.23>.
- Ainsworth, R.B., Vakarelov, B.K., Nanson, R.A., 2011. Dynamic Spatial and Temporal Prediction of Changes in Depositional Processes on Clastic Shorelines: toward Improved Subsurface Uncertainty Reduction and Management, vol. 2, pp. 267–297. <https://doi.org/10.1306/06301010036>.
- Alvarez, T.G., Mann, P., Wood, L.J., 2021. Tectonic evolution of sedimentary basins around the arcuate southeastern margin of the Caribbean plate. In: Bartolini, C. (Ed.), *South America–Caribbean–Central Atlantic plate boundary: Tectonic evolution, basin architecture and petroleum systems: AAPG Memoir 123*, pp. 183–238.
- Amorosi, A., Maselli, V., Trincardi, F., 2016. Onshore to offshore anatomy of a late Quaternary source-to-sink system (Po Plain-Adriatic Sea, Italy). *Earth Sci. Rev.* 153, 212–237. <https://doi.org/10.1016/j.earscirev.2015.10.010>.
- Amos, C.L., Li, M.Z., Chiocci, F.L., La Monica, G.B., Cappucci, S., King, E.H., Corbani, F., 2003. Origin of shore-normal channels from the shoreface of Sable Island, Canada. *J. Geophys. Res. Ocean.* 108.
- Anell, I., Zuchuat, V., Röhnert, A.D., Smyrak-Sikora, A., Buckley, S., Lord, G., Maher, H., Midtkandal, I., Ogata, K., Olaussen, S., Osmundsen, P.T., Braathen, A., 2021. Tidal amplification and along-strike process variability in a mixed-energy paralic system prograding onto a low accommodation shelf, Edgeøya, Svalbard. *Basin Res.* 33, 478–512. <https://doi.org/10.1111/bre.12482>.
- Bentley, S.J., 2003. Wave-Current Dispersal of fine-grained Fluvial Sediments Across Continental Shelves: the Significance of Hyperpynal Plumes.
- Castelle, B., Coco, G., 2012. The morphodynamics of rip channels on embayed beaches. *Cont. Shelf Res.* 43, 10–23.
- Castillo, K., Mann, P., 2021. Structure, stratigraphy, and hydrocarbon potential of the easternmost part of the Eastern Venezuelan foreland basin. In: Bartolini, C. (Ed.), *South America–Caribbean–Central Atlantic plate boundary: Tectonic evolution, basin architecture, and petroleum systems: AAPG Memoir 123*, pp. 591–620.
- Cattaneo, A., Correggiari, A., Langone, L., Trincardi, F., 2003. The late-Holocene Gargano subaqueous delta, adriatic shelf: sediment pathways and supply fluctuations. *Mar. Geol.* 193, 61–91. [https://doi.org/10.1016/S0025-3227\(02\)00614-X](https://doi.org/10.1016/S0025-3227(02)00614-X).
- Cattaneo, A., Trincardi, F., Asioli, A., Correggiari, A., 2007. The Western Adriatic shelf clinoform: energy-limited bottomset. *Cont. Shelf Res.* 27, 506–525. <https://doi.org/10.1016/j.csr.2006.11.013>.
- Chen, S., Steel, R., Olariu, C., Li, S., 2018. Growth of the paleo-orinoco shelf-margin prism: process regimes, delta evolution, and sediment budget beyond the shelf edge. *GSA Bull.* 130, 35–63.
- Chen, S., Steel, R., Olariu, C., Li, S., 2017. Growth of the paleo-Orinoco shelf-margin prism: Process regimes, delta evolution, and sediment budget beyond the shelf edge 1–29. <https://doi.org/10.1130/B31553.1>.
- Collins, D.S., Johnson, H.D., Allison, P.A., Damit, A.R., 2018. Mixed process, humid-tropical, shoreline-shelf deposition and preservation: middle miocene–modern baram Delta Province, Northwest borneo. *J. Sediment. Res.* 88, 399–430. <https://doi.org/10.2110/jsr.2018.19>.
- Correggiari, A., Cattaneo, A., Trincardi, F., 2005. The modern Po Delta system: Lobe switching and asymmetric prodelta growth. *Mar. Geol.* 222–223, 49–74. <https://doi.org/10.1016/j.margeo.2005.06.039>.
- Cummings, D., Dalrymple, R., Choi, K., Jin, J., 2015. *The tide-dominated Han River Delta, Korea: Geomorphology, Sedimentology, and Stratigraphic Architecture*. Elsevier.
- Dasgupta, S., Buatois, L.A., Mángano, M.G., 2016. Living on the edge: evaluating the impact of stress factors on animal-sediment interactions in subenvironments of a shelf-margin delta, the Mayaro Formation, Trinidad. *J. Sediment. Res.* 86, 1034–1066.
- Driscoll, N.W., Karner, G.D., 1999. Three-dimensional quantitative modeling of clinoform development. *Mar. Geol.* 154, 383–398. [https://doi.org/10.1016/S0025-3227\(98\)00125-X](https://doi.org/10.1016/S0025-3227(98)00125-X).
- Dumas, S., Arnott, R.W.C., 2006. Origin of hummocky and swaley cross-stratification - the controlling influence of unidirectional current strength and aggradation rate. *Geology* 34, 1073–1076. <https://doi.org/10.1130/G22930A.1>.
- Escalona, A., Mann, P., 2011. Tectonics, basin subsidence mechanisms, and paleogeography of the Caribbean-South American plate boundary zone. *Mar. Petrol. Geol.* 28, 8–39.
- Friedrichs, C.T., Wright, L.D., 2004. Gravity-driven sediment transport on the continental shelf: implications for equilibrium profiles near river mouths. *Coast. Eng.* 51, 795–811. <https://doi.org/10.1016/j.coastaleng.2004.07.010>.
- Gallop, S.L., Bryan, K.R., Coco, G., Stephens, S.A., 2011. Storm-driven changes in rip channel patterns on an embayed beach. *Geomorphology* 127, 179–188.
- Geleynse, N., Storms, J.E.A., Walstra, D.-J.R., Jagers, H.R.A., Wang, Z.B., Stive, M.J.F., 2011. Controls on river delta formation; insights from numerical modelling. *Earth Planet Sci. Lett.* 302, 217–226.
- Hampson, G.J., 2010. Sediment dispersal and quantitative stratigraphic architecture across an ancient shelf. *Sedimentology* 57, 96–141. <https://doi.org/10.1111/j.1365-3091.2009.01093.x>.
- Hampson, G.J., Premwichein, K., 2017. Sedimentologic character of ancient muddy subaqueous-deltaic clinoforms: down Cliff Clay Member, Bridport Sand Formation, Wessex Basin, U.K. *J. Sediment. Res.* 87, 951–966.
- Hampson, G.J., Storms, J.E.A., 2003. Geomorphological and sequence stratigraphic variability in wave-dominated, shoreface-shelf parasequences. *Sedimentology* 50, 667–701. <https://doi.org/10.1046/j.1365-3091.2003.00570.x>.
- Helland-Hansen, W., Hampson, G.J., 2009. Trajectory analysis: concepts and applications. *Basin Res.* 21, 454–483. <https://doi.org/10.1111/j.1365-2117.2009.00425.x>.
- Jerolmack, D.J., Swenson, J.B., 2007. Scaling relationships and evolution of distributary networks on wave-influenced deltas. *Geophys. Res. Lett.* 34, L23402.
- Jerrett, R.M., Bennie, L.I., Flint, S.S., Greb, S.F., 2016. Extrinsic and intrinsic controls on mouth bar and mouth bar complex architecture: examples from the Pennsylvanian (Upper Carboniferous) of the central Appalachian Basin, Kentucky, USA. *Bulletin* 128, 1696–1716.
- Klausen, T.G., Torland, J.A., Eide, C.H., Alaei, B., Olaussen, S., Chiarella, D., 2018. Clinoform development and topset evolution in a mud-rich delta – the Middle Triassic Kobbe Formation, Norwegian Barents Sea. *Sedimentology* 65, 1132–1169. <https://doi.org/10.1111/sed.12417>.
- Kuehl, S.A., Levy, B.M., Moore, W.S., Allison, M.A., 1997. Subaqueous delta of the ganges-brahmaputra river system. *Mar. Geol.* 144, 81–96. [https://doi.org/10.1016/S0025-3227\(97\)00075-3](https://doi.org/10.1016/S0025-3227(97)00075-3).
- Lin, W., Ferron, C., Karner, S., Bhattacharya, J.P., 2020. Classification of paralic channel sub-environments in an ancient system using outcrops: the Cretaceous Gallup system, New Mexico, USA. *J. Sediment. Res.* 90, 1094–1113.
- MacEachern, J. a, Bann, K.L., Bhattacharya, J.P., Howell, Jr.C.D., 2005. *Ichnology of Deltas; Organism Responses to the Dynamic Interplay of Rivers, Waves, Storms, and Tides*. Special Publication - Society for Sedimentary Geology.
- Macquaker, J.H.S., Bentley, S.J., Bohacs, K.M., 2010. Wave-enhanced sediment-gravity flows and mud dispersal across continental shelves: reappraising sediment transport

- processes operating in ancient mudstone successions. *Geology* 38, 947–950. <https://doi.org/10.1130/G31093.1>.
- Macquaker, J.H.S., Gawthorpe, R.L., 1993. Mudstone lithofacies in the Kimmeridge Clay Formation, Wessex Basin, southern England: implications for the origin and controls of the distribution of mudstones. *J. Sediment. Petrol.* 63, 1129–1143. <https://doi.org/10.1306/D4267CC1-2B26-11D7-8648000102C1865D>.
- Mann, P., Escalona, A., Castillo, M.V., 2006. Regional geologic and tectonic setting of the Maracaibo supergiant basin, western Venezuela. *Am. Assoc. Petrol. Geol. Bull.* 90, 445–477.
- Michels, K.H., Kudrass, H.R., Hübscher, C., Suckow, A., Wiedicke, M., 1998. The submarine delta of the Ganges-Brahmaputra: Cyclone-dominated sedimentation patterns. *Mar. Geol.* 149, 133–154. [https://doi.org/10.1016/S0025-3227\(98\)00021-8](https://doi.org/10.1016/S0025-3227(98)00021-8).
- Mitchell, N.C., Masselink, G., Huthnance, J.M., Fernandez-Salas, L.M., Lobo, F.J., 2012. Depths of modern coastal sand clinoforms. *J. Sediment. Res.* 82, 469–481. <https://doi.org/10.2110/jsr.2012.40>.
- Mulder, T., Syvitski, J.P.M., Migeon, S., Faugères, J.C., Savoye, B., 2003. Marine hyperpycnal flows: initiation, behavior and related deposits. A review. *Mar. Pet. Geol.* 20, 861–882. <https://doi.org/10.1016/j.marpetgeo.2003.01.003>.
- Myrow, P.M., Southard, J.B., 1996. Tempestite deposition. *J. Sediment. Res.*
- Nanson, R.A., Vakarelov, B.K., Ainsworth, R.B., Williams, F.M., Price, D.M., 2013. Evolution of a Holocene, mixed-process, forced regressive shoreline: the Mitchell River delta, Queensland, Australia. *Mar. Geol.* 339, 22–43.
- Nardin, W., Fagherazzi, S., 2012. The effect of wind waves on the development of river mouth bars. *Geophys. Res. Lett.* 39.
- Nardin, W., Mariotti, G., Edmonds, D.A., Guercio, R., Fagherazzi, S., 2013. Growth of river mouth bars in sheltered bays in the presence of frontal waves. *J. Geophys. Res. Earth Surf.* 118, 872–886.
- Neill, C.F., Allison, M.A., 2005. Subaqueous deltaic formation on the Atchafalaya Shelf, Louisiana. *Mar. Geol.* 214, 411–430. <https://doi.org/10.1016/j.margeo.2004.11.002>.
- Olariu, C., Bhattacharya, J.P., 2006. Terminal distributary channels and Delta front Architecture of river-dominated Delta systems. *J. Sediment. Res.* 76, 212–233. <https://doi.org/10.2110/jsr.2006.026>.
- Osman, A., Steel, R.J., Ramsook, R., Olariu, C., 2024. Impact of wave, tides and fluid mud on fluvial discharge across a compound clinoform (Pliocene Orinoco Delta). *Sedimentology* 71, 1113–1148.
- Osman, A., Steel, R.J., Ramsook, R., Olariu, C., 2023. Impact of wave, tides and fluid mud on fluvial discharge across a compound clinoform (Pliocene Orinoco Delta). *Sedimentology* n/a. <https://doi.org/10.1111/sed.13167>.
- Palamenghi, L., Schwenk, T., Spiess, V., Kudrass, H.R., 2011. Seismostratigraphic analysis with centennial to decadal time resolution of the sediment sink in the Ganges-Brahmaputra subaqueous delta. *Cont. Shelf Res.* 31, 712–730.
- Patruno, S., Hampson, G.J., Jackson, C.A.L., 2015. Quantitative characterisation of deltaic and subaqueous clinoforms. *Earth Sci. Rev.* 142, 79–119. <https://doi.org/10.1016/j.earscirev.2015.01.004>.
- Patruno, S., Helland-Hansen, W., 2018. Clinoforms and clinoform systems: review and dynamic classification scheme for shorelines, subaqueous deltas, shelf edges and continental margins. *Earth Sci. Rev.* 185, 202–233. <https://doi.org/10.1016/j.earscirev.2018.05.016>.
- Pattison, S.A.J., Bruce Ainsworth, R., Hoffman, T.A., 2007. Evidence of across-shelf transport of fine-grained sediments: Turbidite-filled shelf channels in the Campanian Aberdeen Member, Book Cliffs, Utah, USA. *Sedimentology* 54, 1033–1063. <https://doi.org/10.1111/j.1365-3091.2007.00871.x>.
- Pellegrini, C., Maselli, V., Cattaneo, A., Piva, A., Ceregato, A., Trincardi, F., 2015. Anatomy of a compound delta from the post-glacial transgressive record in the Adriatic Sea. *Mar. Geol.* 362, 43–59. <https://doi.org/10.1016/j.margeo.2015.01.010>.
- Pellegrini, C., Patruno, S., Helland-Hansen, W., Steel, R.J., Trincardi, F., 2020. Clinoforms and clinoforms: fundamental elements of basin infill. *Basin Res.* 32, 187–205. <https://doi.org/10.1111/bre.12446>.
- Peng, Y., Olariu, C., Steel, R.J., Peng, Y., Olariu, C., 2020a. Recognizing tide- and wave-dominated compound deltaic clinoforms in the rock record. *Geology* 48, 1149–1153. <https://doi.org/10.1130/G47767.1>.
- Peng, Y., Steel, R.J., Olariu, C., 2017. Transition from storm wave-dominated outer shelf to gullied upper slope: the mid-Pliocene Orinoco shelf margin, South Trinidad. *Sedimentology* 64. <https://doi.org/10.1111/sed.12362>.
- Peng, Y., Steel, R.J., Olariu, C., Li, S., 2020b. Rapid subsidence and preservation of fluvial signals in an otherwise wave-reworked delta front succession: Early-mid Pliocene Orinoco continental-margin growth, SE Trinidad. *Sediment. Geol.* 395, 105555. <https://doi.org/10.1016/j.sedgeo.2019.105555>.
- Peng, Y., Steel, R.J., Rossi, V.M., Olariu, C., 2018a. Mixed-energy process interactions read from a compound-clinoform delta (paleo-orinoco delta, trinidad): preservation of river and tide signals by mud-induced wave damping. *J. Sediment. Res.* 88, 75–90. <https://doi.org/10.2110/jsr.2018.3>.
- Peng, Y., Steel, R.J., Rossi, V.M., Olariu, C., 2018b. Mixed-energy process interactions read from a compound-clinoform delta (paleo-orinoco delta, trinidad): preservation of river and tide signals by mud-induced wave damping. *J. Sediment. Res.* 88, 75–90. <https://doi.org/10.2110/jsr.2018.3>.
- Pirmez, C., Pratson, L.F., Steckler, M.S., 1998. Clinoform development by advection-diffusion of suspended sediment: modeling and comparison to natural systems. *J. Geophys. Res.* 103, 24141. <https://doi.org/10.1029/98JB01516>.
- Plint, A.G., 2014. Mud dispersal across a Cretaceous prodelta: Storm-generated, wave-enhanced sediment gravity flows inferred from mudstone microtexture and microfacies. *Sedimentology* 61, 609–647. <https://doi.org/10.1111/sed.12068>.
- Pontén, A., Plink-Björklund, P., 2007. Depositional environments in an extensive tide-influenced delta plain, Middle Devonian Gauja Formation, Devonian Baltic Basin. *Sedimentology* 54, 969–1006. <https://doi.org/10.1111/j.1365-3091.2007.00869.x>.
- Rey, F.M., Olariu, C., Steel, R.J., 2022. Using the modern Colorado delta to reconstruct the compound clinoforms of the Pliocene Colorado delta. *J. Sediment. Res.* 92, 405–432.
- Roberts, H.H., Sydow, J., 2003. Late Quaternary Stratigraphy and Sedimentology of the Offshore Mahakam Delta, East Kalimantan (Indonesia), vol. 76. *SEPM Spec. Publ.*, pp. 125–145.
- Rossi, V.M., Paterson, N.W., Helland-Hansen, W., Klausen, T.G., Eide, C.H., 2019. Mud-rich delta-scale compound clinoforms in the Triassic shelf of northern Pangea (Havert Formation, south-western Barents Sea). *Sedimentology* 66, 2234–2267. <https://doi.org/10.1111/sed.12598>.
- Rossi, V.M., Steel, R.J., 2016. The role of tidal, wave and river currents in the evolution of mixed-energy deltas: example from the Lajas Formation (Argentina). *Sedimentology* 63, 824–864. <https://doi.org/10.1111/sed.12240>.
- Steel, R., Olsen, T., 2002. Clinoforms, clinoform trajectories and deepwater sands. *Seq. Stratigr. Model. Explor. Prod. Evol. Methodol. Emerg. Model. Appl. Hist.* 22nd Annu. 367–380. <https://doi.org/10.5724/gcs.02.22.0367>.
- Steel, R., Osman, A., Rossi, V.M., Alabdullatif, J., Olariu, C., Peng, Y., Rey, F., 2024. Subaqueous deltas in the stratigraphic record: catching up with the marine geologists. *Earth Sci. Rev.* 256. <https://doi.org/10.1016/j.earscirev.2024.104879>.
- Steel, R.J., Olariu, C., Zhang, J., Chen, S., 2020. What is the topset of a shelf-margin prism? *Basin Res.* 32, 263–278.
- Swenson, J.B., Paola, C., Pratson, L., Voller, V.R., Murray, A.B., 2005. Fluvial and marine controls on combined subaerial and subaqueous delta progradation: morphodynamic modeling of compound-clinoform development. *J. Geophys. Res. Earth Surf.* 110, 1–16. <https://doi.org/10.1029/2004JF000265>.
- Taylor, A.M., Goldring, R., 1993. Description and analysis of bioturbation and ichnofabric. *J. Geol. Soc. London.* 150, 141–148. <https://doi.org/10.1144/gsjgs.150.1.0141>.
- Tesson, M., Posamentier, H.W., Gensous, B., 2000. Stratigraphic organization of late pleistocene deposits of the western part of the Golfe du Lion shelf (Languedoc shelf), Western Mediterranean Sea, using high-resolution seismic and core data. *Am. Assoc. Petrol. Geol. Bull.* 84, 119–150.
- Van Cappelle, M., Stukins, S., Hampson, G.J., Johnson, H.D., 2016. Fluvial to tidal transition in proximal, mixed tide-influenced and wave-influenced deltaic deposits: cretaceous lower sego sandstone, Utah, USA. *Sedimentology* 63, 1333–1361. <https://doi.org/10.1111/sed.12267>.
- Van Der Kolk, D.A., Flaig, P.P., Hasiotis, S.T., 2015. Paleoenvironmental reconstruction of a late cretaceous, muddy, river-dominated polar deltaic system: schrader bluff-prince Creek Formation transition, Shivugak bluffs, north slope of Alaska, USA. *J. Sediment. Res.* 85, 903–936.
- Van Yperen, A.E., Poyatos-Moré, M., Holbrook, J.M., Midtkandal, I., 2020. Internal mouth-bar variability and preservation of subordinate coastal processes in low-accommodation proximal deltaic settings (Cretaceous Dakota Group, New Mexico, USA). *Depos. Rec.* 6, 431–458.
- Walsh, J.P., Nittrouer, C.A., 2009. Understanding fine-grained river-sediment dispersal on continental margins. *Mar. Geol.* 263, 34–45. <https://doi.org/10.1016/j.margeo.2009.03.016>.
- Willis, B.J., 2005. Deposits of tide-influenced river deltas. *River Deltas - Concepts, Models, and Examples*. <https://doi.org/10.2110/pec.05.83.0087>.
- Willis, B.J., Sun, T., Ainsworth, R.B., 2021. Contrasting facies patterns between river-dominated and symmetrical wavedominated delta deposits. *J. Sediment. Res.* 91, 262–295. <https://doi.org/10.2110/JSR.2020.131>.
- Wood, L.J., 2000. Chronostratigraphy and tectonostratigraphy of the Columbus Basin, eastern offshore Trinidad. *Am. Assoc. Petrol. Geol. Bull.* 84, 1905–1928. <https://doi.org/10.1306/8626C721-73B8-11D7-8645000102C1865D>.
- Wright, L.D., Friedrichs, C.T., 2006. Gravity-driven sediment transport on continental shelves: a status report. *Cont. Shelf Res.* 26, 2092–2107. <https://doi.org/10.1016/j.csr.2006.07.008>.
- Zăinescu, F., Vespreamanu-Stroe, A., Anthony, E., Tătu, F., Preoteasa, L., Mateescu, R., 2019. Flood deposition and storm removal of sediments in front of a deltaic wave-influenced river mouth. *Mar. Geol.* 417, 106015.
- Zavala, C., Pan, S.X., 2018. Hyperpycnal flows and hyperpycnites: origin and distinctive characteristics. *Lit. Res.* 30, 1–27.
- Zhang, J., Rossi, V.M., Peng, Y., Steel, R., Ambrose, W., 2019. Revisiting late Paleocene Lower Wilcox deltas, Gulf of Mexico: River-dominated or mixed-process deltas? *Sediment. Geol.* 389, 1–12. <https://doi.org/10.1016/j.sedgeo.2019.05.007>.